A model study of the effective Young's modulus for randomly distributed short-fiber composites

Tom Thorvaldsen

Norwegian Defence Research Establishment (FFI)

25 January 2011

FFI-rapport 2011/00212

105401

P: ISBN 978-82-464-1872-8
E: ISBN 978-82-464-1873-5

Keywords

Youngs modul

Kortfiberkompositt

Matematisk modellering

Fiberorientering

Fiberlengde

Approved by

Einar Willassen	Project Manager
Jan Ivar Botnan	Director

English summary

This report provides an overview of a set of macro-mechanical models for the effective Young's modulus of short fiber composites. Various models are found in the literature with varying complexity, ranging from simple rule of mixtures models to more sophisticated models explicitly taking into account the fiber length and the fiber orientation distribution. The models can be used as a tool for a better understanding of the material properties and material behavior, and are valuable additions to the knowledge obtained from experimental tests. In addition, representative and accurate material models are essential in finite element method (FEM) analyses. FEM modeling is nowadays applied in the design and development of most complex structures.

Sammendrag

Denne rapporten gir en oversikt over et sett med makromekaniske modeller for den effektive verdien av Youngs modul for kortfiberkompositter. Forskjellige modeller med varierende kompleksitet finnes i litteraturen, fra enkle mikseregelmodeller til mer sofistikerte modeller som har eksplisitte uttrykk for fiberlengde og fiberorientering. Modellene kan brukes som et viktig verktøy for bedre å forstå materialenes egenskaper og oppførsel, i tillegg til det som blir observert i eksperimentelle forsøk. I tillegg er representative og nøyaktige materialmodeller essensielt i elementmetodeanalyser. Elementmetodemodellering er per i dag anvendt i design og utvikling av de fleste kompliserte konstruksjoner.

Contents

1	**Introduction**	**7**
2	**Mathematical models**	**8**
2.1	Rule of mixtures models	8
2.1.1	2D models	8
2.1.2	3D models	16
2.2	Fiber length and fiber orientation distribution functions	18
2.3	The laminate analogy approach (LAA)	24
2.4	A laminate approximation model with an explicit FOD function	26
2.5	The laminate-plate method	29
2.5.1	General expressions for the effective properties of the composite	30
2.5.2	The longitudinal Young's modulus	33
2.5.3	Three model cases	34
2.6	The paper physics approach (PPA)	40
3	**Summary and future work**	**42**
	Acknowledgements	**42**
	References	**43**

1 Introduction

In this report, a set of mathematical models for describing the effective properties of short-fiber composite materials has been investigated. Two categories of mathematical models may be defined for this purpose. The first type of models is typically dealing with one fiber embedded in a matrix material, using this unit to describe the overall material properties. The aim is then to establish expressions for the interface between the fiber and the matrix, and to model the fiber stress and the interface shear stress distributions of the fiber. Both analytical expressions and numerical simulations are employed. The second type of models are more concerned with finding average values for the material, so that the composite can be described *macroscopically* by an isotropic or, more generally, an anisotropic material model. This category typically includes rule of mixtures models, as well as more sophisticated variants. In addition, this latter category of models distinguishes between aligned and randomly distributed short-fiber composites. A random distribution may in many situations be more adequate.

This report is restricted to only considering macro-mechanical models for randomly oriented short-fiber composites. Different approaches for describing the effective properties have been suggested and presented in the literature. The main interest here is to establish the parameter values for describing the elastic properties of the composite material. These values are required in, for example, finite element method (FEM) analyses. One main parameter is the modulus of elasticity, i.e. Young's modulus, in the direction of the applied load. In this report, the modeling approaches where algebraic expressions are available will be covered.

Some of the models in this survey are implemented in Matlab, showing the elastic properties as a function of the fiber volume fraction. For the simplest models, the influence of fiber length and fiber orientation is included implicitly. For the more sophisticated models, explicit expressions for length variation and fiber orientation are included. Hence, the number of possible parameters that can be tuned depends on the complexity of each model.

With the models at hand, we are able to run a lot more test cases than would be feasible experimentally. Mathematical modeling hence becomes an additional tool in the analysis. It should, however, be mentioned that no experimental tests are performed to verify or support any of the mathematical models. Future studies on discontinuous fiber composites will, however, naturally include an experimental part.

Parts of the contents of this report has already been presented at the 14th European Conference on Composite Materials [1]. Future work, which is also expressed in the conference proceeding paper, will investigate whether the short-fiber models are applicable to model nanocomposites. For that reason, some references to papers where short-fiber models are applied for nanocomposites are included here.

2 Mathematical models

2.1 Rule of mixtures models

The first type of models for describing the macro-mechanical properties of short-fiber composites is based on the assumption that the fibers are randomly oriented, and that the overall material properties can be expressed by some weighted sum of the material properties of the constituents of the composite material, that is, the fibers and the matrix. If at all included in the model, the fiber length variation is assumed to be expressed by some average, or mean, value. This type is often referred to as *rule of mixtures* models.

The final expressions for the composite material are algebraic relations, established from experimental tests. The Young's modulus, and in some cases also the Poisson's ratio, is given. Macroscopically the material is now treated as isotropic. Also, assuming linear elastic properties, a linear stress-strain relation can be defined for the composite.

Most expressions are presented for two-dimensional (2D) cases. Due to the microscopic anisotropy, it is often more complicated to perform tests for 3D cases. Some of the works found in the literature for this model type are, however, also described for 3D cases. Models describing the properties and assumptions in more detail will be shown next.

2.1.1 2D models

One of the earliest studies on randomly oriented short-fiber composites is found in the paper by Cox [2], which considered modeling of cellulose fiber materials, i.e. paper. His theory is often referred to as the shear-lag analysis or the paper physics approach, see e.g. [3]. The paper physics approach is based on the fundamental point of calculating the force from fibers crossing an arbitrary line in the test specimen. The Young's modulus is then found from the final expression of the force. The paper physics approach is more thoroughly described in Section 2.6.

Based on a discussion of the orientation of the fibers, and by assuming that the material at hand macroscopically can be described as isotropic, Cox suggested a very simple model for the effective elasticity modulus,

$$E_C = \frac{V_f E_f}{3} + (1 - V_f) E_m . \qquad (2.1)$$

In the above expression, V_f is the fiber volume fraction, E_f is the Young's modulus of the fibers, and E_m is the Young's modulus of the matrix. From assuming a linear elastic material, and knowing the effective shear modulus, G_C, of the composite, the Poisson's ratio may be found from

$$\nu_C = \frac{E_C}{2G_C} - 1, \tag{2.2}$$

Many later models are based on the pioneer work by Cox.

A similar model as the Cox model for describing the elastic properties of paper has been presented by Horio and Onogi [4]. Instead of including the elastic modulus of the fibers and the matrix, they applied the elastic modulus in the direction of the paper production machine and in the cross direction, that is, $E_{\parallel}$ and $E_{\perp}$, respectively. The elastic mean value through the angular distribution is given as,

$$E_C = (E_{\parallel} E_{\perp})^{1/2}. \tag{2.3}$$

A slightly more sophisticated model for randomly oriented reinforcements in thin resin films, i.e. a 2D orientation distribution, may be established. The elasticity modulus and shear modulus of the composite can be expressed by employing a relation containing the material properties of the two main constituents of the composite, see e.g. [5-8],

$$E_C = \frac{3}{8} E_L + \frac{5}{8} E_T, \tag{2.4}$$

$$G_C = \frac{1}{8} E_L + \frac{1}{4} E_T, \tag{2.5}$$

where E_L and E_T are the longitudinal and transverse modulus of an *aligned* short-fiber composite. The moduli can be expressed mathematically,

$$E_L = \frac{1 + (2l/d)\eta_L V_f}{1 - \eta_L V_f} E_m, \tag{2.6}$$

$$E_T = \frac{1 + 2\eta_T V_f}{1 - \eta_T V_f} E_m, \tag{2.7}$$

where

$$\eta_L = \frac{(E_f / E_m) - 1}{(E_f / E_m) + 2(l/d)}, \tag{2.8}$$

$$\eta_T = \frac{(E_f / E_m) - 1}{(E_f / E_m) + 2}. \tag{2.9}$$

The relations in (2.6) and (2.7) are referred to as the Halpin-Tsai equations for aligned short-fiber composites. In the above expressions, V_f is the fiber volume fraction, E_f is the elastic modulus of the fibers, E_m is the elastic modulus of the matrix, l is the fiber length, and d is the fiber diameter. The *aspect ratio* is defined as the fiber length divided by the fiber diameter (l/d). For the randomly oriented short-fiber composite under consideration, the fiber aspect ratio and fiber volume fraction is the same as in the corresponding aligned short-fiber composite. Furthermore, from assuming an isotropic, linear elastic material, the Poisson ratio is given in (2.2). Also, note that, in this latter rule of mixtures model, the fiber length and the fiber diameter are both explicitly included in the model, and hence the geometric properties of all fibers are assumed equal. Typically some kind of average, or mean, value is applied for the fiber length. This may not be the case for "real-life" composites. Note that the moduli E_L and E_T can alternatively be determined experimentally, and put directly into (2.4) and (2.5).

The Halpin-Tsai equations have become one of the commonly used models for describing the effective properties of randomly oriented short-fiber composites. For example, Fu and Lauke [3] employed this model for comparison with their extended laminated analogy approach (LAA) model, further described in Section 2.5.3.1. Moreover, these equations have also been used for other materials, for instance in the work by Qian *et al*. [6] for estimating the elasticity modulus of a composite consisting of multi-walled carbon nanotubes (MWCNTs) dispersed in a polystyrene (PS) matrix. In this case the nanotubes play the role of the fibers, where d is the outer tube diameter. As reported in the review paper by Coleman and co-workers [9], the Halpin-Tsai equations are known to fit experimental data for low fiber volume fraction composites. For high volume fractions the stiffness is, however, underestimated.

Coleman *et al.* [9] also showed a rule of mixtures model, which is based on the pioneer work by Cox [2]. One general expression is established, which include discontinuous fiber composites with either aligned fibers or randomly oriented fibers. This rule of mixtures expression is written as,

$$E_C = \eta_0 \eta_1 E_f V_f + (1 - V_f) E_m, \tag{2.10}$$

where $\eta_0 = 1$ for aligned fibers, $\eta_0 = 3/8$ for fibers uniformly distributed in a plane, and $\eta_0 = 1/5$ for 3D uniformly distribution [10]. Furthermore [11],

$$\eta_1 = 1 - \frac{\tanh\left(\frac{al}{d}\right)}{\left(\frac{al}{d}\right)}, \tag{2.11}$$

With

$$a = \sqrt{\frac{-3E_m}{2E_f \ln V_f}}\,. \tag{2.12}$$

In the above expressions, E_f and E_m is the Young's modulus of the fiber and the matrix, respectively. Moreover, l is the fiber length, d is the diameter, and V_f is the fiber volume fraction.

A similar model as the previous one, is also shown by Fu and Lauke [12],

$$E_C = \chi_1 \chi_2 E_f V_f + (1 - V_f) E_m, \tag{2.13}$$

where the χ_1 and χ_2 generally are function expressions for the fiber orientation and the fiber length, respectively, but may also be set to constant values. Such functions will be described in more detail in later sections. They are often applied in combination with the laminate analogy approach, see Section 2.3, where an in-plane fiber orientation is presumed. Moreover, the product of the factors, that is, $\chi_1 \chi_2$, is denoted the fiber efficiency factor.

Christensen and Waals [13] and Christensen [14] presented expressions for the effective stiffness for randomly oriented fiber composites based on a geometric average process. In their model, the fibers are assumed to have any orientation in a given plane. The short-fibers are assumed to be sufficiently long, so that they can be treated as continuous fibers, and such that the end effects may be neglected. For the 2D case, the effective properties can be written as

$$\begin{aligned} E_C &= \frac{1}{\mu_1}(\mu_1^2 - \mu_2^2) \\ \nu_C &= \frac{\mu_2}{\mu_1} \end{aligned} \tag{2.14}$$

where

$$\begin{aligned} \mu_1 &= \frac{3}{8}E_{11} + \frac{G_{12}}{2} + \frac{(3 + 2\nu_1 + 3\nu_1^2)G_{23}K_{23}}{2(G_{23} + K_{23})} \\ \mu_2 &= \frac{1}{8}E_{11} - \frac{G_{12}}{2} + \frac{(1 + 6\nu_1 + \nu_1^2)G_{23}K_{23}}{2(G_{23} + K_{23})} \end{aligned} \tag{2.15}$$

The quantities in the above expressions are based on and taken from the work by Hashin and Rosen [15], Hashin [16;17], and Hill [18;19],

$$E_{11} = V_f E_f + (1-V_f)E_m + 4V_f(1-V_f)G_m \left[\frac{(\nu_f - \nu_m)^2}{\frac{(1-V_f)G_m}{k_f + G_f/3} + \frac{V_f G_m}{k_m + G_m/3} + 1} \right]$$

$$\nu_1 = \nu_{12} = (1-V_f)\nu_m + V_f \nu_f + \frac{V_f(1-V_f)(\nu_f - \nu_m)\left(\frac{G_m}{k_m + G_m/3} - \frac{G_m}{k_f + G_f/3} \right)}{\frac{(1-V_f)G_m}{k_f + G_f/3} + \frac{V_f G_m}{k_m + G_m/3} + 1}$$

$$K_{23} = k_m + \frac{G_m}{3} + \frac{V_f}{\frac{1}{k_f - k_m + (1/3)(G_f - G_m)} + \frac{1-V_f}{k_m + (4/3)G_m}} \qquad (2.16)$$

$$G_{12} = G_m \left[\frac{G_f(1+V_f) + G_m(1-V_f)}{G_f(1-V_f) + G_m(1+V_f)} \right]$$

$$G_{23} = G_m \left[1 + \frac{V_f}{\frac{G_m}{G_f - G_m} + \frac{[k_m + (7/3)G_m](1-V_f)}{2(k_m + (4/3)G_m)}} \right]$$

$$k_m = \frac{E_m}{3(1-2\nu_m)}$$

$$k_f = \frac{E_f}{3(1-2\nu_f)}$$

Note that the expression for the transverse shear modulus, G_{23}, is a lower bound. An exact value is not available. Furthermore, in case the fibers are very stiff compared to the matrix material, the expressions in (2.16) may be simplified. Under certain restrictions, given in the referred papers, it may be shown that,

$$
\begin{aligned}
E_{11} &\cong V_f E_f + (1-V_f)E_m + \frac{4V_f(1-V_f)G_m(\nu_f-\nu_m)^2}{1+\dfrac{V_f G_m}{k_m+G_m/3}} \\
\nu_1 &\cong (1-V_f)\nu_m + V_f\nu_f + \frac{V_f(1-V_f)(\nu_f-\nu_m)\left(\dfrac{G_m}{k_m+G_m/3}\right)}{1+\dfrac{V_f G_m}{k_m+G_m/3}} \\
K_{23} &\cong k_m + \frac{G_m}{3} + \frac{V_f(k_m+(4/3)G_m)}{1-V_f} \\
G_{12} &\cong \frac{(1+V_f)}{(1-V_f)}G_m \\
G_{23} &\cong G_m\left[1+\frac{2V_f(k_m+(4/3)G_m)}{[k_m+(7/3)G_m](1-V_f)}\right]
\end{aligned}
\tag{2.17}
$$

Please note that the expressions in (2.16) and (2.17) also can be applied for 3D cases, see Section 2.1.2 for more details.

Another model for 2D cases is presented by Weng and Sun [20]. This model is also referred to and applied in the paper by Chon and Sun [21]. In this case, the effective Young's modulus for the composite is computed from

$$
\begin{aligned}
E_C &= \frac{1}{\mu_1}(\mu_1^2-\mu_2^2) \\
\nu_C &= \frac{\mu_2}{\mu_1}
\end{aligned}
\tag{2.18}
$$

where

$$
\begin{aligned}
\mu_1 &= \frac{3}{8}E_{11} + \frac{G_{12}}{2} + \frac{(3+2\nu_1+3\nu_1^2)G_{23}K_{23}}{2(G_{23}+K_{23})} \\
\mu_2 &= \frac{1}{8}E_{11} - \frac{G_{12}}{2} + \frac{(1+6\nu_1+\nu_1^2)G_{23}K_{23}}{2(G_{23}+K_{23})}
\end{aligned}
\tag{2.19}
$$

And

$$E_{11} = \frac{V_f E_f (1+R)^2}{1+(E_f R / E_m)} + \left[1 - V_f (1+R)\right] E_m$$

$$\nu_1 = \left[1 - V_f (1+R)\right] \nu_m + V_f (1+R) \frac{\nu_f E_m + R \nu_m E_f}{R E_f + E_m}$$

$$K_{23} = k_m + \frac{G_m}{3} + \frac{V_f}{\dfrac{1}{k_f - k_m + (G_f - G_m)/3} + \dfrac{1 - V_f}{k_m + 4G_m/3}}$$

$$G_{12} = G_m \left[\frac{G_f (1+V_f) + G_m (1-V_f)}{G_f (1-V_f) + G_m (1+V_f)} \right] \tag{2.20}$$

$$G_{23} = G_m \left[1 + \frac{V_f}{\dfrac{G_m}{G_f - G_m} + \dfrac{[k_m + (7/3)G_m](1-V_f)}{2(k_m + (4/3)G_m)}} \right]$$

$$k_m = \frac{E_m}{3(1-2\nu_m)}$$

$$k_f = \frac{E_f}{3(1-2\nu_f)}$$

In the above expressions, the modulus E_{11} and the Poisson number ν_1 are presented in the paper, whereas the other expressions are taken from the paper by Christensen and Waals [13], which again is based on the work by Hashin and Rosen [15], Hashin [16;17], and Hill [18;19]. Hence, this model is very similar to the Christensen-Waals model. In (2.20), the parameter

$$R \equiv \frac{l}{l_f} - 1, \tag{2.21}$$

where $l = l_f + l_m$ is the sum of the length of the matrix, l_m, and the length of the fiber, l_f. In their model a "unit" is defined, consisting of a cylindrical short-fiber embedded in and surrounded by a cylindrically shaped matrix tube. Hence, this theory also takes into account the length of the fibers. The rest of the parameters are given earlier. The Weng-Sun model is in their paper [20] compared to other models and also experimental results, and is said to be the most suitable model for the given experimental data.

For comparison, the rule of mixtures model shown in the paper by Christensen and Waals [13] is included,

$$E_C = V_f E_f + (1 - V_f) E_m . \tag{2.22}$$

This model may at first be a natural choice. It is, however, stated in their paper that this model produces absurd results. It does neither take into account the random orientation nor the fiber-matrix interaction effects, which is the case for the Cox model and the more sophisticated models. A similar expression is also often applied for the Poisson's ratio of the composite.

Most of the above models for the effective Young's modulus of randomly distributed short-fiber composites have been implemented in Matlab for a varying fiber volume fraction, V_f. However, only those models where the elastic modulus is a function of the elastic properties of the constituent materials, are displayed in the plot, as shown in Figure 2.1. In all cases, $E_m = 1000000$ and $E_f = 26.25E_m$. Moreover, for the Halpin-Tsai model the aspect ratio is set to 10. For the (advanced) Christensen-Waals model and the Weng-Sun model, $\nu_m = 0.35$ and $\nu_f = 0.20$. Finally, for the Weng-Sun model, $l = 2l_f$. Please note that because the different models require different material parameters, the model results may not be directly comparable. For example, by choosing a different value for l in the Weng-Sun model, the curve will change, while the remaining models, which do not explicitly depend on this quantity (or have a similar input parameter), will not be altered. Nevertheless, from the curves we observe that the Young's modulus when applying the Christensen-Waals rule of mixtures model (in green) gives a much steeper increase and higher stiffness compared to the other models. The more sophisticated Christensen-Waals model (in red) is very close to the model where the Halpin-Tsai expressions (in magenta) are applied. The other models overall predict a lower increase in the Young's modulus as a function of the fiber volume fraction, and lower stiffness values for large fiber volume fractions.

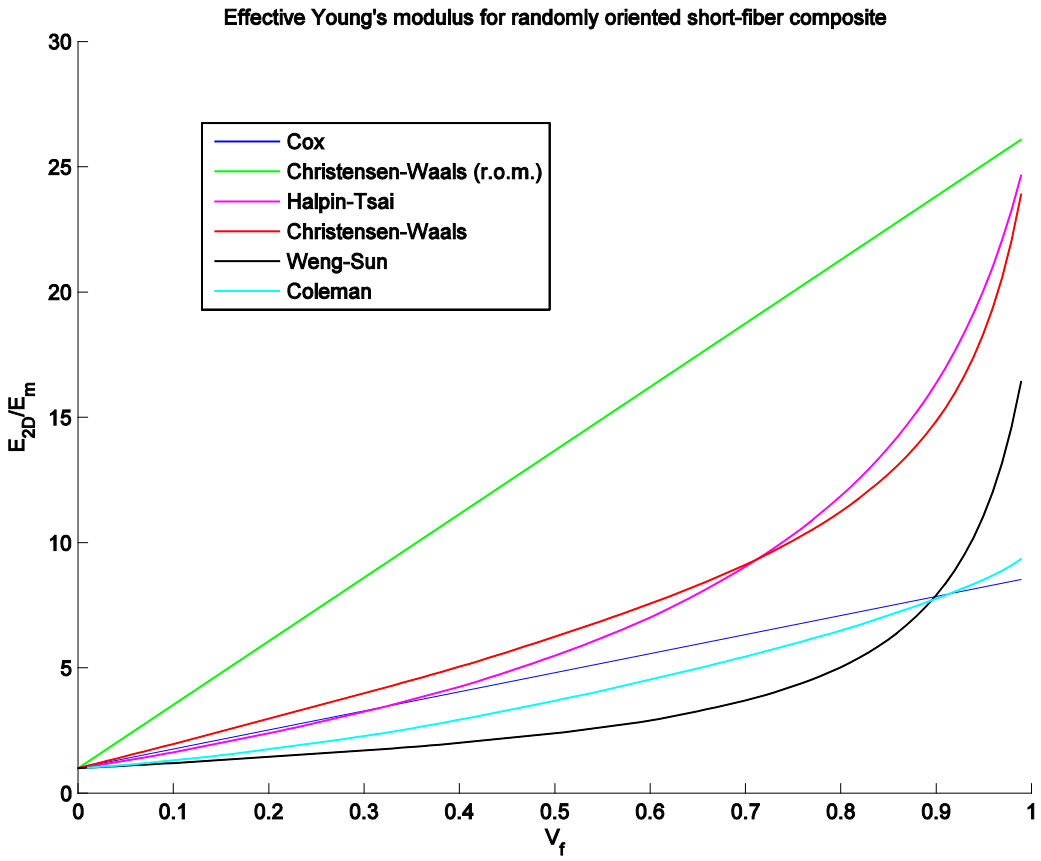

Figure 2.1 Effective Young's modulus for the composite material versus fiber volume fraction, 2D case. All values are normalized with the Young's modulus of the matrix material.

2.1.2 3D models

As described in the previous section, the paper by Cox [2] presents one of the earliest models for randomly oriented short-fiber composites. For 3D orientation of the fibers, based on the description of the 2D case presented above, he suggested that

$$E_C = \frac{V_f E_f}{6} + (1 - V_f) E_m, \tag{2.23}$$

where V_f, as before, is the fiber volume fraction, E_f is the Young's modulus of the fibers, and E_m the Young's modulus of the matrix. In the same way as for the 2D case, the Poisson ratio is given in (2.2). Breton *et al.* [22] used this model also for estimating the elasticity modulus of multi-walled carbon nanotubes (MWCNT) embedded in an epoxy resin. In this case, the MWCNTs take the role of the short-fibers.

Another model for the effective elasticity modulus of short-fiber composites, with a random orientation in 3D, have been presented by Lavengood and Goettler [7],

$$E_C = \frac{1}{5}E_L + \frac{4}{5}E_T \,. \tag{2.24}$$

The longitudinal and transverse elasticity moduli in the latter expression can be expressed by the Halpin-Tsai expressions in (2.6) and (2.7). In [7], the corresponding shear modulus for 3D cases is not explicitly given, neither is the Poisson's ratio. Hence, the paper does not provide enough information for describing all the material properties, especially needed in mathematical and numerical modeling. Moreover, Kardos [8] referred to this model in his paper, stating that more work need to be done for 3D random orientation to obtain a general format, as is the case for 2D cases.

Fidelus *et al.* [23] have presented a rule of mixtures model for prediction of Young's modulus for 3D randomly dispersed carbon nanotube composites,

$$E_C = \lambda E_{NT} V_{NT} + E_m (1 - V_{NT}) \,. \tag{2.25}$$

As Fidelus and co-workers used this model for carbon nanotubes, V_{NT} in their model refer to the volume fraction of the tubes, and E_{NT} and E_m denote the elastic modulus for the nanotubes and the matrix, respectively. Moreover, λ is here the so-called Krenchel's coefficient, which for 3D randomly oriented rods with high aspect ratio, may be set to a constant value. However, a similar expression should also be applicable to short-fiber composites.

As mentioned in the previous section, Christensen and Waals [13] and Christensen [14] presented expressions for the effective stiffness of randomly oriented fiber composites, both for 2D and 3D cases. For the 3D case, the effective properties of the composite can be written as,

$$\begin{aligned} E_C &= \frac{[E_{11} + (4\nu_1^2 + 8\nu_1 + 4)K_{23}][E_{11} + (4\nu_1^2 - 4\nu_1 + 1)K_{23} + 6(G_{12} + G_{23})]}{3[2E_{11} + (8\nu_1^2 + 12\nu_1 + 7)K_{23} + 2(G_{12} + G_{23})]} \\ \nu_C &= \frac{E_{11} + (4\nu_1^2 + 16\nu_1 + 6)K_{23} - 4(G_{12} + G_{23})}{4E_{11} + (16\nu_1^2 + 24\nu_1 + 14)K_{23} + 4(G_{12} + G_{23})} \end{aligned} \tag{2.26}$$

It can also be shown, see [14], that in this case

$$\begin{aligned} G_C &= \frac{1}{15}[E_{11} + (1 - 2\nu_1)^2 K_{23} + 6(G_{12} + G_{23})] \\ k_C &= \frac{1}{9}[E_{11} + 4(1 + \nu_1)^2 K_{23}] \end{aligned} \tag{2.27}$$

The parameters in (2.26) and (2.27) are given in (2.16). In a similar way as in the 2D case, for stiff fibers (compared to the matrix), the parameters are given in (2.17).

Weng and Sun [20] also presented a 3D variant for the effective properties of 3D randomly oriented short-fiber composites. The expressions for the effective Young's modulus and Poisson's ratio are taken from the Christensen-Waals model in (2.26). As for the 2D case, described in the previous section, the parameters involved are given in (2.20).

Finally, the Coleman model [9] presented in (2.10) may also be applied for 3D uniformly distribution. As already mentioned in Section 2.1.1, the only change is that η_0 (now) equals 1/5.

Some of the 3D models for the effective Young's modulus of randomly distributed short-fiber composites have been implemented in Matlab, and plotted as shown in Figure 2.2. In the same way as for the 2D case in the previous section, the different models require different material parameters, and hence the model results may not be directly comparable.

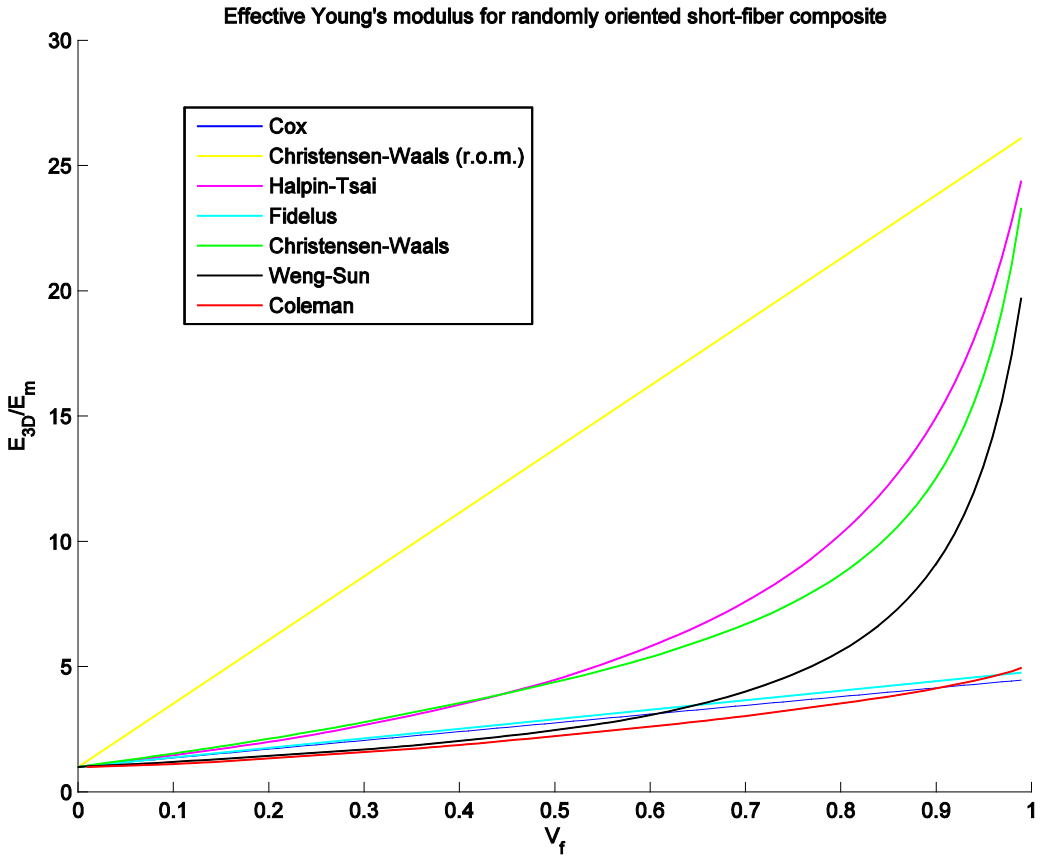

Figure 2.2 Effective Young's modulus for the composite material versus fiber volume fraction, 3D case. All values are normalized with the Young's modulus of the matrix material.

2.2 Fiber length and fiber orientation distribution functions

In the previous section, rule of mixtures models for the effective properties of randomly distributed short-fiber composites have been presented. In these models, the composite properties are established from assuming that all orientations are equally probable. Moreover, the fiber length and diameter, defining the aspect ratio of the fibers, are assumed to be constant. To extend

this a bit further, functions have been presented in the literature to also include variations in fiber length and fiber orientation. The variation in fiber length is denoted the *fiber length distribution* (FLD) function, whereas the variation in fiber orientation is called the *fiber orientation distribution* (FOD) function. Some commonly applied FLD and FOD functions will be presented next.

Fu and Lauke [3;24;25] put up a two-parameter Weibull distribution for modeling the FLD,

$$f(l) = (m/n)(l/n)^{m-1} \exp[-(l/n)^m], \tag{2.28}$$

for $l > 0$, where n and m are shape parameters. Another form of the Weibull distribution function is the so-called Tung distribution,

$$f(l) = abl^{b-1} \exp(-al^b), \tag{2.29}$$

also valid for $l > 0$. Setting $b = m$ and $a = n^{-m}$ into the Tung distribution, gives the Weibull distribution function. The cumulative distribution function, can then be given as

$$F(l) = \int_0^l f(l)dl = 1 - \exp(-al^b), \tag{2.30}$$

and the mean fiber length as

$$l_{\text{mean}} = \int_0^\infty lf(l)dl = a^{-1/b}\Gamma(1/b+1). \tag{2.31}$$

The Tung distribution has recently been applied by Fu *et al.* [26] for analyses of carbon nanotubes polymer composites.

For the FOD, Fu and Lauke [3;24;25] used a two-parameter function proposed by Xia *et al.* [27],

$$g(\theta) = \frac{\{\sin(\theta)\}^{2p-1}\{\cos(\theta)\}^{2q-1}}{\int_{\theta_{\min}}^{\theta_{\max}} \{\sin(\theta)\}^{2p-1}\{\cos(\theta)\}^{2q-1} \mathrm{d}\theta}. \tag{2.32}$$

The angle θ is defined as the angle between the fiber direction and the direction of the applied load. During production, the fibers are typically distorted, moved, and broken, for example in an injection molding process, and hence the fiber length and the orientation of the fibers vary in a short-fiber composite. Although considering a 3D distribution, the fiber orientation can, as an approximation, still be modeled by the single angle θ describing the direction of the fiber within the composite plane. An algebraic expression for the integral of the above FOD function is, however, only available for certain fiber orientation ranges.

Fu and Lauke [3;28] presented the same probability functions as described in [3;24;25] for characterization of the anisotropy of the elastic modulus of misaligned short-fiber reinforced polymers (SFRP). In addition to the above two functions, they included another fiber orientation distribution function $g(\phi)$, based on the work by Xia *et al.* [27], for the variation in another direction than considered by the $g(\theta)$ function in (2.32),

$$g(\phi) = \frac{\{\sin(\phi/2)\}^{2s-1}\{\cos(\phi/2)\}^{2t-1}}{\int_{\phi_{\min}}^{\phi_{\max}} \{\sin(\phi/2)\}^{2s-1}\{\cos(\phi/2)\}^{2t-1}\mathrm{d}\theta}. \tag{2.33}$$

While the angle θ is defined as the angle between the 1-axis (the axis in the direction of the externally applied load) and the local fiber axis, the angle ϕ is defined as the angle between the 2-axis and the projection of the fiber on to the 2-3-axes plane. A sketch of the coordinate directions is found in [28]. Note that in the latter expression the angle varies from 0 to π. Moreover, a similar expression for this angle range can be expressed also for the $g(\theta)$ function in (2.32). In that case, to satisfy the periodic conditions, p must equal q, and s must be equal to t.

Chin *et al*. [29] presented two possible approaches for modeling the FLD. The first approach was the two-parameter Weibull distribution, which is expressed as

$$f(l) = \frac{c}{b}\left(\frac{l}{b}\right)^{c-1} \exp[-(l/b)^c]. \tag{2.34}$$

Here, b and c are shape parameters. From this, one may find an expression for the mean fiber length, which by definition is equal to the expected fiber length,

$$l_{\text{mean}} = l_{\text{exp}} = b\Gamma\left(\frac{1}{c}+1\right), \tag{2.35}$$

where Γ is the gamma function. The function in (2.34) is, in fact, identical to the function presented by Fu and Lauke [3;24;25], given in (2.28), with $c = m$ and $b = n$.

The second function presented by Chin *et al.* for the FLD is a log-normal distribution function, which may be expressed as,

$$f(l) = \frac{1}{\sqrt{2\pi}sl}\exp[-(\ln l - \mu)^2/2s^2], \tag{2.36}$$

where s and μ are model parameters, and l is, as before, the fiber length. Note that the fiber length, l, in the denominator of the above expression is missing in Equation (7) in [29]; this is probably a misprint.

In this case, the mean fiber length (and the expected fiber length) may be expressed as,

$$l_{\text{mean}} = l_{\text{exp}} = \exp[\mu + \frac{s^2}{2}]. \tag{2.37}$$

Moreover, the most probable length (modal length) may be expressed as

$$l_{\text{mod}} = \exp[\mu - s^2]. \tag{2.38}$$

From rearranging the expressions in (2.37) and (2.38), the model parameters may be expressed as,

$$\begin{aligned} s &= \sqrt{\frac{2}{3}(\ln l_{\text{mean}} - \ln l_{\text{mod}})} \\ \mu &= \frac{2\ln l_{\text{mean}} + \ln l_{\text{mod}}}{3} \end{aligned} \tag{2.39}$$

For the FOD, Chin *et al.* [29] proposed a modified version of the model by Kacir *et al.* [30]. To be more specific, the probability density function and the cumulative distribution function of Chin *et al.* read

$$\begin{aligned} g(\theta) &= \frac{\lambda e^{-\lambda\theta}}{1 - e^{-\frac{\pi}{2}\lambda}} \\ F(\theta) &= \frac{1 - e^{-\lambda\theta}}{1 - e^{-\frac{\pi}{2}\lambda}} \end{aligned} \tag{2.40}$$

respectively. It is seen that $F(\theta)$, which is the accumulated percent of fibers oriented between zero and $\pm\theta$, satisfies the requirement $F(\frac{\pi}{2}) = 1$, which means that the relative probability of the fiber angle to be between 0 and $\pi/2$ equals unity. That is, since all fibers are oriented in the range from 0 to $\pi/2$, the cumulative distribution function must equal 100 percent for all values of λ.This is, however, not the case for the FOD function proposed by Kacir *et al.* [30], expressed as,

$$\rho(\theta) = \lambda e^{-\lambda\theta}. \tag{2.41}$$

That is, the orientation distribution function is not normalized, and therefore it is only suitable for cases where λ is large.

The integral of the Chin *et al.* FOD function in (2.40) is

$$\int_{\theta_{\min}}^{\theta_{\max}} g(\theta)d\theta = \int_{\theta_{\min}}^{\theta_{\max}} \frac{\lambda e^{-\lambda\theta}}{1-e^{-\frac{\pi}{2}\lambda}} d\theta = \frac{1}{1-e^{-\frac{\pi}{2}\lambda}}\left[e^{-\lambda\theta_{\min}} - e^{-\lambda\theta_{\max}}\right]. \tag{2.42}$$

For an angle variation of θ from zero to $\pi/2$, the latter integral becomes unity.

To get a better understanding of how the fiber orientation is affected by the values of λ, the probability density function and the cumulative distribution function in (2.40) are plotted in Figure 2.3 and Figure 2.4, respectively, for different values of λ. As can be seen, a large value of λ indicates that the fibers are aligned, whereas a small value of λ indicates a random distribution. Similar plots are shown in [29].

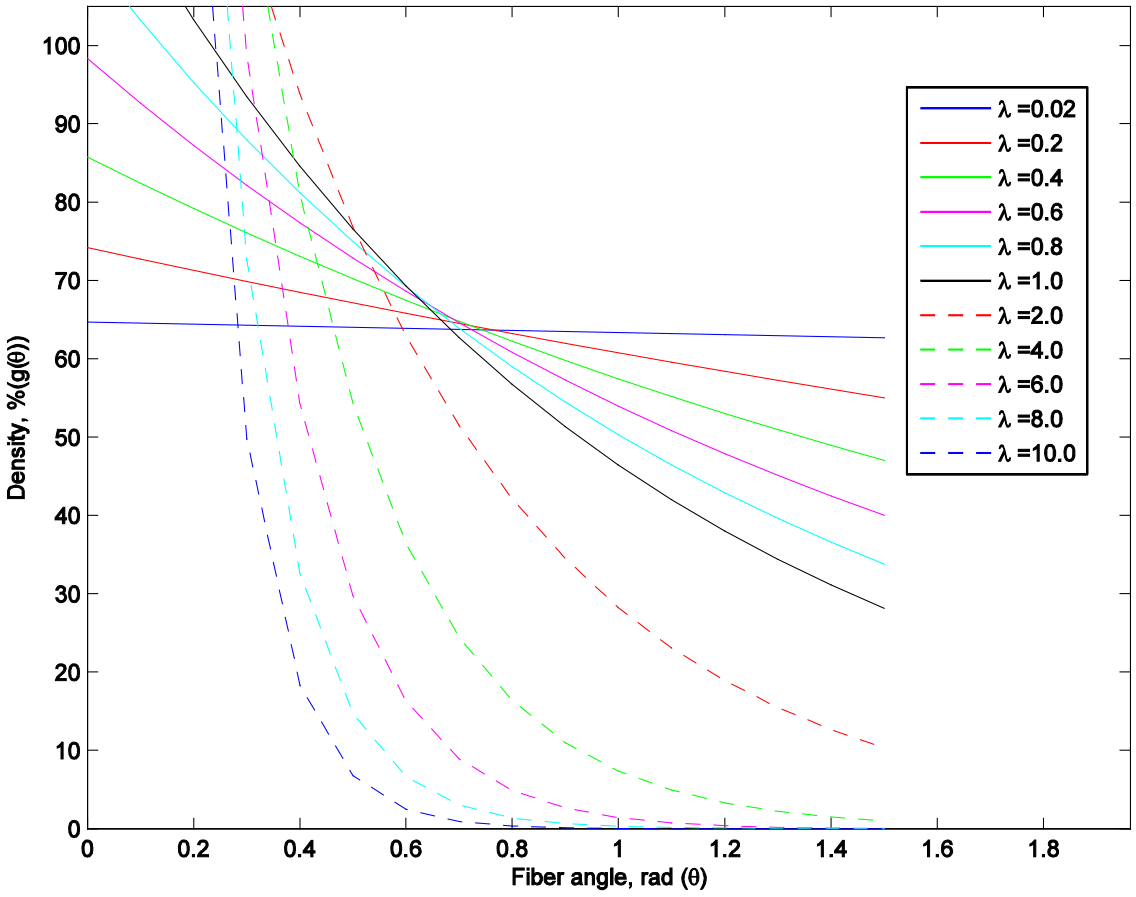

Figure 2.3 Orientation density curves for various values of λ.

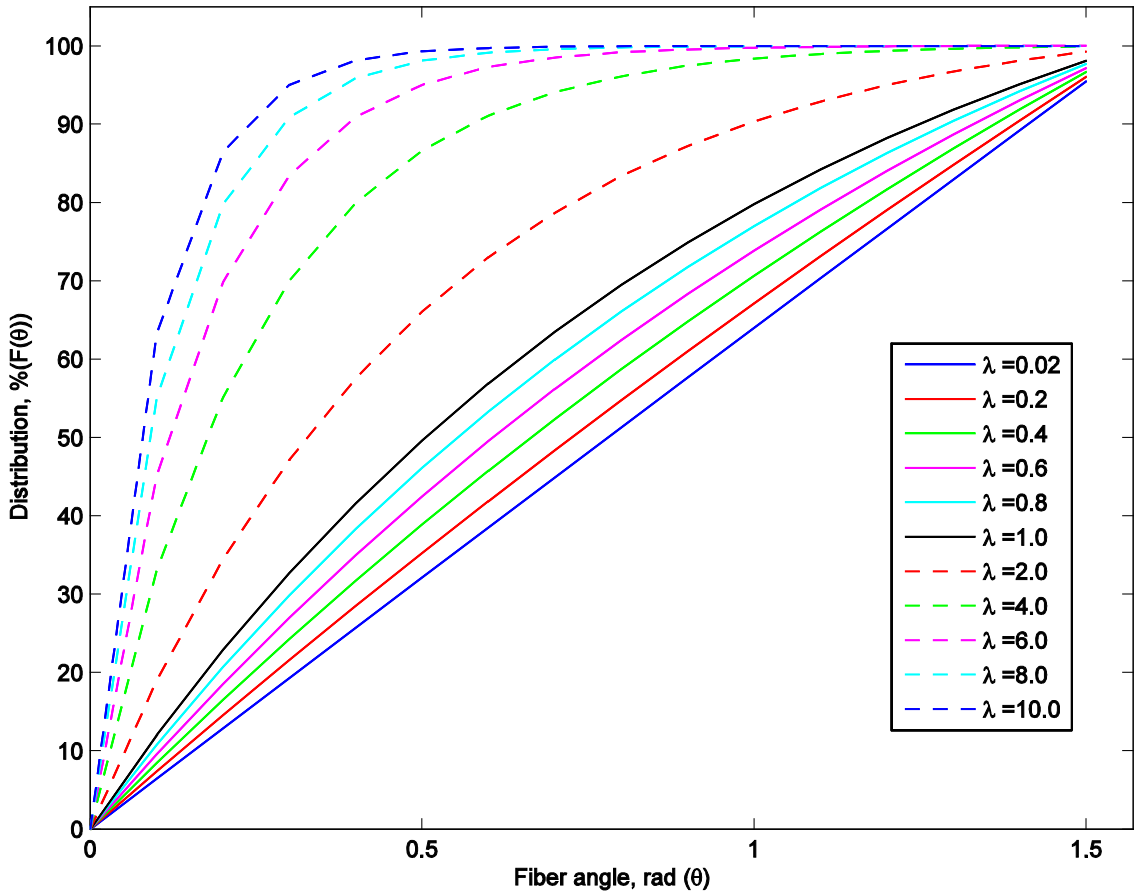

Figure 2.4 Cumulative distribution of fibers for various values of λ.

Chen and Cheng [31] used a slightly more complex theory for estimating the elasticity properties of a plane and transversely isotropic material case. They adopted the single exponential fiber orientation function proposed by Kacir *et al.* [30], defined by (2.41). In addition to the fiber distribution, the elastic moduli of the short-fiber composite were assumed to be a function of the elastic moduli of the constituent materials, the fiber volume fraction, and the aspect ratio. Different expressions for the components of the stiffness matrix were applied in cases of planar orientation of the fibers and transversely isotropic situations. In the latter case, the distribution function $\rho(\theta)$ was assumed axisymmetric with respect to one major axis of the test specimen considered, and the material then became transversely isotropic in planes normal to this axis. Unfortunately, all parameters are not defined in the paper, and hence it is difficult to implement this model.

In later sections, some models, where the above distribution functions are applied in estimating the effective Young's modulus for the composite, will be described.

2.3 The laminate analogy approach (LAA)

A *laminate analogy approach* has been employed in many papers for estimating the effective elasticity modulus of short-fiber composites. One of the earliest approaches, and probably the first, was proposed by Halpin and co-workers [32-34]. In this approach, the short-fiber composite is modeled mathematically as a laminated composite. General laminate theory is applied, see e.g. [5].

The effective properties of the quasi-isotropic short-fiber composite can in this model be expressed as,

$$E_C = \frac{4U_5(U_1 - U_5)}{U_1}, \tag{2.43}$$

$$\nu_C = \frac{U_1 - 2U_5}{U_1}, \tag{2.44}$$

$$G_C = U_5 . \tag{2.45}$$

Here,

$$\begin{aligned} U_1 &= \frac{3Q_{11} + 3Q_{22} + 2Q_{12} + 4Q_{66}}{8} \\ U_5 &= \frac{Q_{11} + Q_{22} - 2Q_{12} + 4Q_{66}}{8} \end{aligned} \tag{2.46}$$

with

$$\begin{aligned} Q_{11} &= \frac{E_L}{1 - \nu_{LT}\nu_{TL}} \\ Q_{22} &= \frac{E_T}{1 - \nu_{LT}\nu_{TL}} \\ Q_{12} &= \frac{E_L\nu_{TL}}{1 - \nu_{LT}\nu_{TL}} \\ Q_{66} &= G_{LT} \end{aligned} \tag{2.47}$$

In the above expressions, E_L is the longitudinal elasticity modulus and E_T is the transverse elasticity modulus, ν_{LT} is the major Poisson's ratio and ν_{TL} is the minor Poisson's ratio, and finally, G_{LT} is the in-plane shear modulus.

The elasticity moduli and the shear modulus are in this model calculated from the Halpin-Tsai expressions, which are expressed as

$$E_L = \frac{1+(2l/d)\eta_L V_f}{1-\eta_L V_f} E_m, \tag{2.48}$$

$$E_T = \frac{1+2\eta_T V_f}{1-\eta_T V_f} E_m, \tag{2.49}$$

and

$$G_{LT} = \frac{1+\eta_S V_f}{1-\eta_S V_f} G_m, \tag{2.50}$$

where

$$\eta_L = \frac{(E_f/E_m)-1}{(E_f/E_m)+2(l/d)}, \tag{2.51}$$

$$\eta_T = \frac{(E_f/E_m)-1}{(E_f/E_m)+2}, \tag{2.52}$$

and

$$\eta_S = \frac{(G_f/G_m)-1}{(G_f/G_m)+1}. \tag{2.53}$$

As can be seen, the shear modulus may be expressed in a similar way as the elasticity moduli; for convenience, we have repeated the expressions for the elasticity moduli here (already given in (2.6) - (2.9)). Moreover, for the longitudinal Poisson's ratio a rule of mixture expression is used, resulting in

$$\nu_{LT} = \nu_f V_f + \nu_m (1-V_f). \tag{2.54}$$

The minor Poisson's ratio may be expressed as,

$$\nu_{TL} = \frac{\nu_{LT} E_T}{E_L}. \tag{2.55}$$

The Halpin *et al.* model presented in this section and the 3D rule of mixtures models introduced in Section 2.1.2 are shown in Figure 2.5. The same set of material parameter values are used for all models in the plot. As also mentioned in the discussion of Figure 2.1, the length of the (short) fibers are not explicitly included in all the models, and therefore the results are not directly comparable. However, as can be seen in the plot, the Halpin *et al.* model (blue, dashed line) is very close to the Halpin-Tsai rule of mixtures model (in magenta).

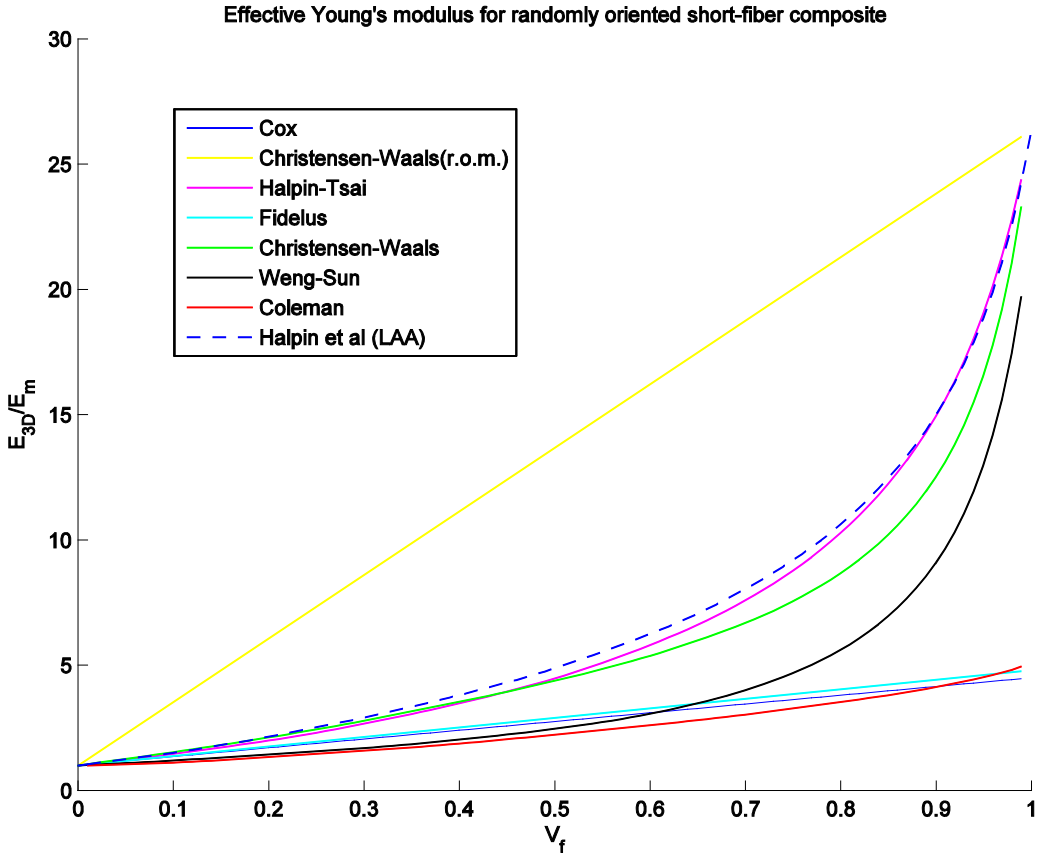

Figure 2.5 Effective Young's modulus for the composite material versus fiber volume fraction, 3D case. All values are normalized with the Young's modulus of the matrix material.

2.4 A laminate approximation model with an explicit FOD function

The LAA described in Section 2.3, which here will be referred to as the original LAA, is based on the Halpin-Tsai expressions developed and established from empirical test results. In this model, the fiber aspect ratio, i.e. the fiber length divided by the fiber diameter, is set to some constant value, and the variation in fiber orientation is implicitly contained in the model. As already mentioned, models that explicitly include distribution functions for fiber length and fiber orientation have been presented, and a model described by Choy *et al.* [35], where a FOD function is explicitly included, will now be described.

In the Choy *et al.* model, the material properties are given referred to the local fiber system for each ply in a layered composite. These axes generally make angles with respect to the (fixed)

global coordinate system for the composite. The relationship between the components of the stiffness matrix in the global, or off-axis, system and the local fiber system, can be expressed as

$$\begin{aligned}
Q_{11}^{'} &= U_1 + U_2\cos 2\theta + U_3\cos 4\theta \\
Q_{22}^{'} &= U_1 - U_2\cos 2\theta + U_3\cos 4\theta \\
Q_{12}^{'} &= U_4 - U_3\cos 4\theta \\
Q_{66}^{'} &= U_5 - U_3\cos 4\theta \\
Q_{16}^{'} &= \frac{1}{2}U_2\sin 2\theta + U_3\sin 4\theta \\
Q_{26}^{'} &= \frac{1}{2}U_2\sin 2\theta - U_3\sin 4\theta
\end{aligned} \tag{2.56}$$

where

$$\begin{aligned}
U_1 &= \frac{3Q_{11} + 3Q_{22} + 2Q_{12} + 4Q_{66}}{8} \\
U_2 &= \frac{Q_{11} - Q_{22}}{2} \\
U_3 &= \frac{Q_{11} + Q_{22} - 2Q_{12} - 4Q_{66}}{8} \\
U_4 &= \frac{Q_{11} + Q_{22} - 6Q_{12} - 4Q_{66}}{8} \\
U_5 &= \frac{U_1 - U_4}{2}
\end{aligned} \tag{2.57}$$

Please note that the expressions for the components referred to the local fiber system, Q_{ij}, are not explicitly given in [35]. However, it may be assumed that the standard laminate theory, as described in e.g. [5], and with the components given in (2.47), is applied.

Now, using the syntax in [35], referring to [36;37], a set of modified rule of mixtures expressions for unidirectional lamina can be written. The Young's modulus along the fiber direction, E_1, and the longitudinal Poisson's ratio, ν_{12}, of the unidirectional composite may be expressed as

$$E_1 = \frac{\eta_1 V_f E_{f1} + V_m E_m}{\eta_1 V_f + V_m}, \tag{2.58}$$

$$\nu_{12} = \frac{\eta_1 V_f \nu_{f12} + V_m \nu_m}{\eta_1 V_f + V_m}. \tag{2.59}$$

The longitudinal shear modulus, G_6, the transverse shear modulus, G_4, and the plain strain bulk modulus, k, may be written

$$G_6 = \frac{V_f + \eta_6 V_m}{\frac{V_f}{G_{f6}} + \frac{\eta_6 V_m}{G_m}}, \tag{2.60}$$

$$G_4 = \frac{V_f + \eta_4 V_m}{\frac{V_f}{G_{f4}} + \frac{\eta_4 V_m}{G_m}}, \tag{2.61}$$

$$k = \frac{V_f + \eta_k V_m}{\frac{V_f}{k_f} + \frac{\eta_k V_m}{k_m}}. \tag{2.62}$$

Finally, the transverse Young's moduli are related to the above parameters,

$$E_2 = E_3 = \frac{4kG_4}{k + mG_4}, \tag{2.63}$$

where

$$m = 1 + \frac{4k\nu_{12}^2}{E_1}. \tag{2.64}$$

Moreover,

$$\eta_1 = \frac{1 - V_f}{\frac{\beta\alpha}{\beta\alpha - \tanh\beta\alpha} - V_f}, \tag{2.65}$$

with $\beta = [2G_m\sqrt{V_f} / (E_f(1-\sqrt{\nu_f}))]^{1/2}$ and $\alpha = l/d$, and

$$\begin{aligned} \eta_4 &= \frac{3 - 4\nu_m + \frac{G_m}{G_{f4}}}{4(1-\nu_m)} \\ \eta_6 &= \frac{1 + G_m / G_{f6}}{2} \\ \eta_k &= \frac{1 + \frac{G_m}{k_f}}{2(1-\nu_m)} \end{aligned} \tag{2.66}$$

In all the above expressions for this model, f refers to the fibers, whereas m refers to the matrix. From a stress-strain relation for the laminated composite, the stiffness matrix may be expressed as

$$\bar{A}_{ij} = \frac{1}{h}\int_{-h/2}^{h/2} Q_{ij}^{'} dh^{'}, \quad i, j = 1, 2, 6, \tag{2.67}$$

where h is the thickness of the laminate and $dh^{'} = \frac{h\lambda e^{-\lambda\theta}}{1-e^{-\lambda\pi/2}} d\theta$, with the FOD function explicitly included.

Substituting (2.56) into (2.67), we get

$$\begin{aligned}
\bar{A}_{11} &= U_1 + U_2 V_1 + U_3 V_2 \\
\bar{A}_{22} &= U_1 - U_2 V_1 + U_3 V_2 \\
\bar{A}_{12} &= U_4 - U_3 V_2 \\
\bar{A}_{66} &= U_5 - U_3 V_2 \\
\bar{A}_{16} &= \bar{A}_{26} = 0
\end{aligned} \tag{2.68}$$

Here,

$$V_1 = \frac{1}{h}\int_{-h/2}^{h/2} \cos 2\theta dh^{'} = \frac{\lambda^2(1+e^{-\lambda\pi/2})}{(\lambda^2+4)(1-e^{-\lambda\pi/2})}, \tag{2.69}$$

and

$$V_2 = \frac{1}{h}\int_{-h/2}^{h/2} \cos 4\theta dh^{'} = \frac{\lambda^2}{\lambda^2+16}. \tag{2.70}$$

The in-plane elastic moduli can then be calculated from the in-plane stiffness. Moreover, from assuming uniform out-of-plane stresses, also the out-of-plane elastic moduli can be calculated from the above expressions. More details can be found in the paper.

2.5 The laminate-plate method

As an even further development of the laminate approximation approach described in the previous sections, the modeling can be extended by also explicitly including a fiber length distribution (FLD) function. One such model, which is based on the original laminate analogy approach (LAA), is referred to as the *laminate-plate method* [3;24;25;29]. The real composite is in this model, as in the original LAA, replaced by a layered short-fiber model composite. The terms set by the authors for the real composite and the model composite will be adopted in this report.

In the laminate-plate method, it is assumed that the overall fiber orientation can be described by a probability function for the *in-plane* fiber orientation. Hence, in the *simulated composite* it is assumed that no fibers are pointing out of the plane. The loading direction is in the in-plane direction. Thus, the out-of-plane direction is perpendicular to the loading plane. The simulated, or model, composite is first defined by a set of laminae, each with a given fiber length. Hence, the fiber length is constant for each laminate. Second, each laminate with a given fiber length is again split up in to a set of laminae, where each laminate has a given fiber orientation. In this way, all fibers in each laminate have the same length *and* orientation. From this, models for *aligned* short-fiber composites with a constant fiber length, such as the Halpin-Tsai model, may be applied in the modeling, see Section 2.1.1. A sketch of the simulated composite is shown in Figure 2 in [3].

A laminate-plate model, very similar to the one just described, has also been presented by Xia *et al.* [27]. In their model, the laminate is build up of a core layer and two (outer) skin layers. The skin layers are split up into layers with fibers of equal length and with in-plane fiber orientation. Each layer is then again split up into a set of laminae with in-plane unidirectional fiber orientation. The core layer, on the other hand, is first split up into a set of laminae, with a given fiber length for each laminate, but with out-of-plane fiber orientation. Next, each laminate is again split up into laminae with unidirectional fiber orientation projected onto the in-plane plane. A sketch of the model composite in this case is shown in Figure 2 in [27]. This particular model will, however, not be further discussed in this report.

In the next section, general expressions are given for estimating the effective Young's modulus using the laminated-plate method in [3;24;25;29]. These expressions contain the longitudinal elasticity modulus, as well as a fiber length distribution function (FLD) and a fiber orientation distribution function (FOD). The expressions applied for the longitudinal elasticity modulus will be given in Section 2.5.2. The expressions for the distribution functions are already given in Section 2.2. To recapitulate, the FLD and FOD functions given in (2.29) and (2.32), respectively, are applied by Fu and Lauke [3;24;25] in estimating the Young's modulus of a misaligned short-fiber composite. If including these probability functions, the fiber length and the fiber orientation can explicitly be taken into account. Similarly, the FLD and FOD functions from (2.36) and (2.40), respectively, are employed by Chin *et al.* [29] for the same purpose; Kacir *et al.* [30] used the same FLD, but the FOD was replaced by the function in (2.41). The laminate-plate method may hence be seen as an extension of the models for the effective properties of a randomly oriented short-fiber composite described in sections 2.1, 2.3, and 2.4.

2.5.1 General expressions for the effective properties of the composite

In the same way as described in Section 2.4, material properties are given referred to the local fiber system for each ply in a layered composite. These axes generally make angles with respect to the global coordinate system for the complete composite.

The relationship between the components of the stiffness matrix in the global, or off-axis, system and the local fiber system, can be expressed as [5],

$$\begin{pmatrix} Q_{11}^{'} \\ Q_{22}^{'} \\ Q_{12}^{'} \\ Q_{66}^{'} \\ Q_{16}^{'} \\ Q_{26}^{'} \end{pmatrix} = \begin{pmatrix} m^4 & n^4 & 2m^2n^2 & 4m^2n^2 \\ n^4 & m^4 & 2m^2n^2 & 4m^2n^2 \\ m^2n^2 & m^2n^2 & m^4+n^4 & -4m^2n^2 \\ m^2n^2 & m^2n^2 & -2m^2n^2 & (m^2-n^2)^2 \\ m^3n & -mn^3 & mn^3-m^3n & 2(mn^3-m^3n) \\ mn^3 & -m^3n & m^3n-mn^3 & 2(m^3n-mn^3) \end{pmatrix} \times \begin{pmatrix} Q_{11} \\ Q_{22} \\ Q_{12} \\ Q_{66} \end{pmatrix}. \tag{2.71}$$

Here, $m = \cos\theta$ and $n = \sin\theta$, and the components of the right hand side vector Q_{ij} are given in (2.47).

From the simulated composite, the overall stiffness properties are found by summing the contribution from each layer, where the layer material properties are multiplied by the layer thickness. However, when introducing continuous distribution functions for the variation in fiber length and fiber orientation, the overall stiffness matrix is expressed by an integral, that is [3],

$$\overline{A}_{ij} = \int_{l_{\min}}^{l_{\max}} \int_{\theta_{\min}}^{\theta_{\max}} Q_{ij}^{'} f(l) g(\theta) dl d\theta, \tag{2.72}$$

where $0 \le l_{\min} \le l \le l_{\max} < \infty$, and $0 \le \theta_{\min} \le \theta \le \theta_{\max} \le \pi/2$.

Inserting the expressions in (2.71) into (2.72)**,** the integrand of each component of the stiffness matrix, $\overline{A}_{ij}$, can be written as a product of a fiber length dependent function and a fiber orientation dependent function. This yields,

$$\begin{aligned} \overline{A}_{11} = & \int_{l_{\min}}^{l_{\max}} \frac{E_L^2}{E_L - \nu_{LT}^2 E_T} f(l) dl \int_{\theta_{\min}}^{\theta_{\max}} \cos^4\theta g(\theta) d\theta \\ & + \int_{l_{\min}}^{l_{\max}} \frac{E_L E_T}{E_L - \nu_{LT}^2 E_T} f(l) dl \int_{\theta_{\min}}^{\theta_{\max}} \sin^4\theta g(\theta) d\theta \\ & + \int_{l_{\min}}^{l_{\max}} \frac{2\nu_{LT} E_T E_L}{E_L - \nu_{LT}^2 E_T} f(l) dl \int_{\theta_{\min}}^{\theta_{\max}} \cos^2\theta \sin^2\theta g(\theta) d\theta \\ & + \int_{l_{\min}}^{l_{\max}} 4G_{LT} f(l) dl \int_{\theta_{\min}}^{\theta_{\max}} \cos^2\theta \sin^2\theta g(\theta) d\theta \end{aligned} \tag{2.73}$$

$$\begin{aligned}\overline{A}_{22} = &\int_{l_{\min}}^{l_{\max}} \frac{E_L^2}{E_L - \nu_{LT}^2 E_T} f(l)dl \int_{\theta_{\min}}^{\theta_{\max}} \sin^4\theta g(\theta)d\theta \\ &+ \int_{l_{\min}}^{l_{\max}} \frac{E_L E_T}{E_L - \nu_{LT}^2 E_T} f(l)dl \int_{\theta_{\min}}^{\theta_{\max}} \cos^4\theta g(\theta)d\theta \\ &+ \int_{l_{\min}}^{l_{\max}} \frac{2\nu_{LT} E_T E_L}{E_L - \nu_{LT}^2 E_T} f(l)dl \int_{\theta_{\min}}^{\theta_{\max}} \cos^2\theta \sin^2\theta g(\theta)d\theta \\ &+ \int_{l_{\min}}^{l_{\max}} 4G_{LT} f(l)dl \int_{\theta_{\min}}^{\theta_{\max}} \cos^2\theta \sin^2\theta g(\theta)d\theta\end{aligned} \tag{2.74}$$

$$\begin{aligned}\overline{A}_{12} = &\int_{l_{\min}}^{l_{\max}} \frac{E_L^2}{E_L - \nu_{LT}^2 E_T} f(l)dl \int_{\theta_{\min}}^{\theta_{\max}} \cos^2\theta \sin^2\theta g(\theta)d\theta \\ &+ \int_{l_{\min}}^{l_{\max}} \frac{E_L E_T}{E_L - \nu_{LT}^2 E_T} f(l)dl \int_{\theta_{\min}}^{\theta_{\max}} \cos^2\theta \sin^2\theta g(\theta)d\theta \\ &+ \int_{l_{\min}}^{l_{\max}} \frac{\nu_{LT} E_T E_L}{E_L - \nu_{LT}^2 E_T} f(l)dl \int_{\theta_{\min}}^{\theta_{\max}} \cos^4\theta g(\theta)d\theta \\ &+ \int_{l_{\min}}^{l_{\max}} \frac{\nu_{LT} E_T E_L}{E_L - \nu_{LT}^2 E_T} f(l)dl \int_{\theta_{\min}}^{\theta_{\max}} \sin^4\theta g(\theta)d\theta \\ &- \int_{l_{\min}}^{l_{\max}} 4G_{LT} f(l)dl \int_{\theta_{\min}}^{\theta_{\max}} \cos^2\theta \sin^2\theta g(\theta)d\theta\end{aligned} \tag{2.75}$$

$$\begin{aligned}\overline{A}_{66} = &\int_{l_{\min}}^{l_{\max}} \frac{E_L^2}{E_L - \nu_{LT}^2 E_T} f(l)dl \int_{\theta_{\min}}^{\theta_{\max}} \cos^2\theta \sin^2\theta g(\theta)d\theta \\ &+ \int_{l_{\min}}^{l_{\max}} \frac{E_L E_T}{E_L - \nu_{LT}^2 E_T} f(l)dl \int_{\theta_{\min}}^{\theta_{\max}} \cos^2\theta \sin^2\theta g(\theta)d\theta \\ &- \int_{l_{\min}}^{l_{\max}} \frac{2\nu_{LT} E_T E_L}{E_L - \nu_{LT}^2 E_T} f(l)dl \int_{\theta_{\min}}^{\theta_{\max}} \cos^2\theta \sin^2\theta g(\theta)d\theta \\ &+ \int_{l_{\min}}^{l_{\max}} G_{LT} f(l)dl \int_{\theta_{\min}}^{\theta_{\max}} \cos^4\theta g(\theta)d\theta \\ &- \int_{l_{\min}}^{l_{\max}} 2G_{LT} f(l)dl \int_{\theta_{\min}}^{\theta_{\max}} \cos^2\theta \sin^2\theta g(\theta)d\theta \\ &+ \int_{l_{\min}}^{l_{\max}} G_{LT} f(l)dl \int_{\theta_{\min}}^{\theta_{\max}} \sin^4\theta g(\theta)d\theta\end{aligned} \tag{2.76}$$

The stiffness components above are applicable to different longitudinal elasticity modulus functions, as well as various fiber length and fiber orientation distribution functions. Furthermore, the effective composite engineering tensile properties are given by [3]

$$\overline{E}_{11} = \frac{\overline{A}_{11}\overline{A}_{22} - \overline{A}_{12}^2}{\overline{A}_{22}}, \tag{2.77}$$

$$\overline{E}_{22} = \frac{\overline{A}_{11}\overline{A}_{22} - \overline{A}_{12}^2}{\overline{A}_{11}}, \tag{2.78}$$

$$\overline{G}_{12} = \overline{A}_{66}, \tag{2.79}$$

$$\overline{\nu}_{12} = \overline{E}_{11}\frac{\overline{A}_{12}}{\overline{A}_{11}\overline{A}_{22} - \overline{A}_{12}^2} = \frac{\overline{A}_{12}}{\overline{A}_{22}}. \tag{2.80}$$

As an extension of the integral expression in (2.72), Fu and Lauke [28] included an additional function for the fiber orientation distribution, see Section 2.2. In this case, the stiffness matrix for the composite is expressed as

$$\overline{A}_{ij} = \int_{l_{\min}}^{l_{\max}} \int_{\theta_{\min}}^{\theta_{\max}} \int_{\phi_{\min}}^{\phi_{\max}} Q_{ij}^{'} f(l) g(\theta) g(\phi) dl d\theta d\phi, \tag{2.81}$$

with (Θ, Φ) being the loading direction, or the direction of the measurement. This latter model is discussed no further in this report, but more details can be found in the referred paper [3].

2.5.2 The longitudinal Young's modulus

As indicated in the previous section, the two first components of the right hand side vector, $\mathbf{Q}$, in (2.71) contain the longitudinal elasticity modulus, E_L. Furthermore, the E_L is generally a function of the fiber length, and must therefore be kept within the integral expression for the composite stiffness matrix. The other material parameters for a unidirectional layer do not depend on the fiber length. Different expressions for the longitudinal Young's modulus are found in the literature, and two of them will be described in the following.

An often employed approach for modeling the longitudinal elasticity modulus is using the Halpin-Tsai expression, given in (2.6). A second approach is applying the shear-lag model by Cox [2], referred to in [3],

$$E_L = E_f\left[1 - \frac{\tanh(\beta l/2)}{\beta l/2}\right]V_f + E_m(1 - V_f), \tag{2.82}$$

where V_f is the fiber volume fraction, E_f is the elasticity modulus of the fibers, E_m is the modulus of the matrix, as before, and

$$\beta = \left[\frac{2\pi G_m}{E_f (\pi r_f^2) \ln(R / r_f)} \right]^{1/2}, \tag{2.83}$$

where G_m is the shear modulus of the matrix, and R is a parameter for the mean separation of the fibers to their length. For a hexagonal packing of the fibers, the logarithmic factor in the denominator can be expressed by

$$\ln\left(\frac{R}{r_f}\right) = \frac{1}{2}\ln\left(\frac{2\pi}{\sqrt{3}V_f}\right), \tag{2.84}$$

while a square packing of the fibers leads to

$$\ln\left(\frac{R}{r_f}\right) = \frac{1}{2}\ln\left(\frac{\pi}{V_f}\right). \tag{2.85}$$

These two model approaches for the longitudinal elasticity modulus will be applied in the following.

2.5.3 Three model cases

With the above general expressions and models for calculating the effective Young's modulus, we now describe three models, namely the Fu-Lauke model [3;24;25], the Chin *et al.* model [29], and the Kacir *et al.* [30] model. In each case, the distribution functions for the fiber length and the fiber orientation define the model. Furthermore, for each model the expression for the longitudinal Young's modulus applied may be varied.

Two variants have been described in the previous section, that is, the Halpin-Tsai expression and the Cox shear-lag expression. Also, taking into account that the shear-lag model includes two different ways of packing the fibers, we then end up with three different expressions for each model, resulting in three different integral expressions for the stiffness matrix. In addition to this, diverse assumptions are made for the solution of the integral.

2.5.3.1 The Fu-Lauke model

The FLD and FOD functions applied in the Fu-Lauke model [3;24;25] are given in (2.29) and (2.32), respectively. These functions are substituted into the expressions for the components of the stiffness matrix in (2.73) to (2.76). Due to the cutting process (from a fiber tow) and the production process of the short-fiber composite, the fiber length is assumed to be in the range from $l_{\min}$ to the cut length of the fibers, $l_{\max}$. For the fiber length dependent integral, an explicit expression for the solution is, however, not available. This is at least the case for Matlab, which is

applied for the calculations; both the FLD function and the longitudinal Young's modulus are generally depending on the fiber length. Moreover, for the fiber orientation dependent integral, a solution is not available for all ranges of fiber orientations. From assuming that the orientation of the fibers are in the range from zero to $\pi/2$, i.e. $0=\theta_{\min}\le\theta\le\theta_{\max}=\pi/2$, the solution of this integral can be explicitly expressed by the Γ function.

Due to the challenges of solving the fiber length dependent integral, E_L is, as a first approximation, assumed to be constant. In this way, we can move the term containing the material parameters outside the integral, and limit the integration to the FLD function. An analytical expression for the integral of the FLD function alone is available, and given in Section 2.2.

The fiber length in the expression for the constant longitudinal elasticity modulus is set to either the mean fiber length or the modal fiber length. In the Fu-Lauke model, the mean fiber length is calculated from

$$l_{\text{mean}}=\int_0^\infty lf(l)dl=a^{-1/b}\Gamma(1/b+1). \tag{2.86}$$

Moreover, the most probable fiber length, i.e. modal length, can be found from setting $\frac{df}{dl}=0$, giving

$$l_{\text{mod}}=\left[\frac{1}{a}-\frac{1}{ab}\right]^{1/b}. \tag{2.87}$$

In the above expressions the shape parameters a and b are tuned such that the modal and mean values are within the fiber length interval, i.e. larger than or equal to $l_{\min}$, and smaller than, or equal to, $l_{\max}$. From these assumptions, the components of the laminate stiffness matrix can be written as

$$\begin{aligned}\bar{A}_{11}=&\frac{E_L^2}{E_L-\nu_{LT}^2E_T}\left[\exp(-al_{\min}^b)-\exp(-al_{\max}^b)\right]\frac{\Gamma(2+q)\Gamma(q+p)}{\Gamma(q)\Gamma(2+q+p)}\\&+\frac{E_LE_T}{E_L-\nu_{LT}^2E_T}\left[\exp(-al_{\min}^b)-\exp(-al_{\max}^b)\right]\frac{\Gamma(2+p)\Gamma(q+p)}{\Gamma(p)\Gamma(2+q+p)}\\&+\frac{2\nu_{LT}E_TE_L}{E_L-\nu_{LT}^2E_T}\left[\exp(-al_{\min}^b)-\exp(-al_{\max}^b)\right]\frac{\Gamma(1+q)\Gamma(1+p)\Gamma(q+p)}{\Gamma(q)\Gamma(p)\Gamma(2+q+p)}\\&+4G_{LT}\left[\exp(-al_{\min}^b)-\exp(-al_{\max}^b)\right]\frac{\Gamma(1+q)\Gamma(1+p)\Gamma(q+p)}{\Gamma(q)\Gamma(p)\Gamma(2+q+p)}\end{aligned} \tag{2.88}$$

$$\begin{aligned}\bar{A}_{22} &= \frac{E_L^2}{E_L - \nu_{LT}^2 E_T}\left[\exp(-al_{\min}^b) - \exp(-al_{\max}^b)\right]\frac{\Gamma(2+p)\Gamma(q+p)}{\Gamma(p)\Gamma(2+q+p)} \\ &+ \frac{E_L E_T}{E_L - \nu_{LT}^2 E_T}\left[\exp(-al_{\min}^b) - \exp(-al_{\max}^b)\right]\frac{\Gamma(2+q)\Gamma(q+p)}{\Gamma(q)\Gamma(2+q+p)} \\ &+ \frac{2\nu_{LT} E_T E_L}{E_L - \nu_{LT}^2 E_T}\left[\exp(-al_{\min}^b) - \exp(-al_{\max}^b)\right]\frac{\Gamma(1+q)\Gamma(1+p)\Gamma(q+p)}{\Gamma(q)\Gamma(p)\Gamma(2+q+p)} \\ &+ 4G_{LT}\left[\exp(-al_{\min}^b) - \exp(-al_{\max}^b)\right]\frac{\Gamma(1+q)\Gamma(1+p)\Gamma(q+p)}{\Gamma(q)\Gamma(p)\Gamma(2+q+p)}\end{aligned} \tag{2.89}$$

$$\begin{aligned}\bar{A}_{12} &= \frac{E_L^2}{E_L - \nu_{LT}^2 E_T}\left[\exp(-al_{\min}^b) - \exp(-al_{\max}^b)\right]\frac{\Gamma(1+q)\Gamma(1+p)\Gamma(q+p)}{\Gamma(q)\Gamma(p)\Gamma(2+q+p)} \\ &+ \frac{E_L E_T}{E_L - \nu_{LT}^2 E_T}\left[\exp(-al_{\min}^b) - \exp(-al_{\max}^b)\right]\frac{\Gamma(1+q)\Gamma(1+p)\Gamma(q+p)}{\Gamma(q)\Gamma(p)\Gamma(2+q+p)} \\ &+ \frac{\nu_{LT} E_T E_L}{E_L - \nu_{LT}^2 E_T}\left[\exp(-al_{\min}^b) - \exp(-al_{\max}^b)\right]\frac{\Gamma(2+q)\Gamma(q+p)}{\Gamma(q)\Gamma(2+q+p)} \\ &+ \frac{\nu_{LT} E_T E_L}{E_L - \nu_{LT}^2 E_T}\left[\exp(-al_{\min}^b) - \exp(-al_{\max}^b)\right]\frac{\Gamma(2+p)\Gamma(q+p)}{\Gamma(p)\Gamma(2+q+p)} \\ &- 4G_{LT}\left[\exp(-al_{\min}^b) - \exp(-al_{\max}^b)\right]\frac{\Gamma(1+q)\Gamma(1+p)\Gamma(q+p)}{\Gamma(q)\Gamma(p)\Gamma(2+q+p)}\end{aligned} \tag{2.90}$$

$$\begin{aligned}\bar{A}_{66} &= \frac{E_L^2}{E_L - \nu_{LT}^2 E_T}\left[\exp(-al_{\min}^b) - \exp(-al_{\max}^b)\right]\frac{\Gamma(1+q)\Gamma(1+p)\Gamma(q+p)}{\Gamma(q)\Gamma(p)\Gamma(2+q+p)} \\ &+ \frac{E_L E_T}{E_L - \nu_{LT}^2 E_T}\left[\exp(-al_{\min}^b) - \exp(-al_{\max}^b)\right]\frac{\Gamma(1+q)\Gamma(1+p)\Gamma(q+p)}{\Gamma(q)\Gamma(p)\Gamma(2+q+p)} \\ &- \frac{2\nu_{LT} E_T E_L}{E_L - \nu_{LT}^2 E_T}\left[\exp(-al_{\min}^b) - \exp(-al_{\max}^b)\right]\frac{\Gamma(1+q)\Gamma(1+p)\Gamma(q+p)}{\Gamma(q)\Gamma(p)\Gamma(2+q+p)} \\ &+ \frac{\nu_{LT} E_T E_L}{E_L - \nu_{LT}^2 E_T}\left[\exp(-al_{\min}^b) - \exp(-al_{\max}^b)\right]\frac{\Gamma(2+p)\Gamma(q+p)}{\Gamma(p)\Gamma(2+q+p)} \\ &+ G_{LT}\left[\exp(-al_{\min}^b) - \exp(-al_{\max}^b)\right]\frac{\Gamma(2+q)\Gamma(q+p)}{\Gamma(q)\Gamma(2+q+p)} \\ &- 2G_{LT}\left[\exp(-al_{\min}^b) - \exp(-al_{\max}^b)\right]\frac{\Gamma(1+q)\Gamma(1+p)\Gamma(q+p)}{\Gamma(q)\Gamma(p)\Gamma(2+q+p)} \\ &+ G_{LT}\left[\exp(-al_{\min}^b) - \exp(-al_{\max}^b)\right]\frac{\Gamma(2+p)\Gamma(q+p)}{\Gamma(p)\Gamma(2+q+p)}\end{aligned} \tag{2.91}$$

In the second case, the elasticity modulus is assumed to be a function of the fiber length, and can hence not be moved outside the integral. Because no analytical solution of the fiber length

dependent integral is available, numerical integration is used. One solution is employing the Simpson's rule, which reads,

$$\int_a^b f(x)dx = \frac{b-a}{6}\left[f(a) + 4f\left(\frac{a+b}{2}\right) + f(b)\right]. \tag{2.92}$$

Please note that for the Fu-Lauke model, only the effective Young's modulus in (2.77) is valid for the real composite, whereas the rest of the expressions are valid for the model composite.

2.5.3.2 The Chin et al model

In the Chin *et al.* [29] model case, the FLD and FOD functions employed are given in (2.36) and (2.40), respectively. For the same reasons as described for the Fu-Lauke model, see Section 2.5.3.1, we assume that the orientation of the fibers are in the range from zero to $\pi/2$, i.e. $0 = \theta_{\min} \le \theta \le \theta_{\max} = \pi/2$. In this way, an explicit solution of the integral is available. Also, no explicit solution of the fiber length dependent integral is available.

As for the Fu-Lauke model in the previous section, we first apply a constant value for E_L, such that the material parameters can be put outside the integral expression. An analytical solution of the integral of the FLD function is given in Section 2.2. For the calculations, the modal and mean fiber length is taken from the Fu-Lauke model. These values are applied in the expression for the longitudinal elasticity modulus, as well as for the parameters for the log-normal distribution function. Hence, the values of a and b are equal to the values in the Fu-Lauke modeling.

From these assumptions, the components of the stiffness matrix in this case become,

$$\begin{aligned}
\bar{A}_{11} = {} & \frac{E_L^2}{E_L - \nu_{LT}^2 E_T}\left\{\frac{1}{2}erf\left[\frac{\sqrt{2}}{2}(\mu - \ln l_{\min})\right] - \frac{1}{2}erf\left[\frac{\sqrt{2}}{2}(\mu - \ln l_{\max})\right]\right\}\frac{\lambda^4 + 16\lambda^2 - 24e^{-\frac{\pi}{2}\lambda} + 24}{(\lambda^4 + 20\lambda^2 + 64)(1 - e^{-\frac{\pi}{2}\lambda})} \\
& + \frac{E_L E_T}{E_L - \nu_{LT}^2 E_T}\left\{\frac{1}{2}erf\left[\frac{\sqrt{2}}{2}(\mu - \ln l_{\min})\right] - \frac{1}{2}erf\left[\frac{\sqrt{2}}{2}(\mu - \ln l_{\max})\right]\right\} \\
& \qquad \frac{24 - e^{-\frac{\pi}{2}\lambda}\lambda^4 - 16e^{-\frac{\pi}{2}\lambda}\lambda^2 - 24e^{-\frac{\pi}{2}\lambda}}{(\lambda^4 + 20\lambda^2 + 64)(1 - e^{-\frac{\pi}{2}\lambda})} \\
& + \frac{2\nu_{LT} E_T E_L}{E_L - \nu_{LT}^2 E_T}\left\{\frac{1}{2}erf\left[\frac{\sqrt{2}}{2}(\mu - \ln l_{\min})\right] - \frac{1}{2}erf\left[\frac{\sqrt{2}}{2}(\mu - \ln l_{\max})\right]\right\}\frac{2\,1 - e^{-\frac{\pi}{2}\lambda}()}{(\lambda^2 + 16)(1 - e^{-\frac{\pi}{2}\lambda})} \\
& + 4G_{LT}\left\{\frac{1}{2}erf\left[\frac{\sqrt{2}}{2}(\mu - \ln l_{\min})\right] - \frac{1}{2}erf\left[\frac{\sqrt{2}}{2}(\mu - \ln l_{\max})\right]\right\}\frac{2(1 - e^{-\frac{\pi}{2}\lambda})}{(\lambda^2 + 16)(1 - e^{-\frac{\pi}{2}\lambda})}
\end{aligned} \tag{2.93}$$

$$\bar{A}_{22} = \frac{E_L^2}{E_L - \nu_{LT}^2 E_T}\left\{\frac{1}{2}erf\left[\frac{\sqrt{2}}{2}(\mu - \ln l_{\min})\right] - \frac{1}{2}erf\left[\frac{\sqrt{2}}{2}(\mu - \ln l_{\max})\right]\right\}$$

$$\frac{24 - e^{-\frac{\pi}{2}\lambda}\lambda^4 - 16e^{-\frac{\pi}{2}\lambda}\lambda^2 - 24e^{-\frac{\pi}{2}\lambda}}{(\lambda^4 + 20\lambda^2 + 64)(1 - e^{-\frac{\pi}{2}\lambda})}$$

$$+ \frac{E_L E_T}{E_L - \nu_{LT}^2 E_T}\left\{\frac{1}{2}erf\left[\frac{\sqrt{2}}{2}(\mu - \ln l_{\min})\right] - \frac{1}{2}erf\left[\frac{\sqrt{2}}{2}(\mu - \ln l_{\max})\right]\right\}\frac{\lambda^4 + 16\lambda^2 - 24e^{-\frac{\pi}{2}\lambda} + 24}{(\lambda^4 + 20\lambda^2 + 64)(1 - e^{-\frac{\pi}{2}\lambda})} \quad (2.94)$$

$$+ \frac{2\nu_{LT} E_T E_L}{E_L - \nu_{LT}^2 E_T}\left\{\frac{1}{2}erf\left[\frac{\sqrt{2}}{2}(\mu - \ln l_{\min})\right] - \frac{1}{2}erf\left[\frac{\sqrt{2}}{2}(\mu - \ln l_{\max})\right]\right\}\frac{2\,1 - e^{-\frac{\pi}{2}\lambda}()}{(\lambda^2 + 16)(1 - e^{-\frac{\pi}{2}\lambda})}$$

$$+ 4G_{LT}\left\{\frac{1}{2}erf\left[\frac{\sqrt{2}}{2}(\mu - \ln l_{\min})\right] - \frac{1}{2}erf\left[\frac{\sqrt{2}}{2}(\mu - \ln l_{\max})\right]\right\}\frac{2(1 - e^{-\frac{\pi}{2}\lambda})}{(\lambda^2 + 16)(1 - e^{-\frac{\pi}{2}\lambda})}$$

$$\bar{A}_{12} = \frac{E_L^2}{E_L - \nu_{LT}^2 E_T}\left\{\frac{1}{2}erf\left[\frac{\sqrt{2}}{2}(\mu - \ln l_{\min})\right] - \frac{1}{2}erf\left[\frac{\sqrt{2}}{2}(\mu - \ln l_{\max})\right]\right\}\frac{2\,1 - e^{-\frac{\pi}{2}\lambda}()}{(\lambda^2 + 16)(1 - e^{-\frac{\pi}{2}\lambda})}$$

$$+ \frac{E_L E_T}{E_L - \nu_{LT}^2 E_T}\left\{\frac{1}{2}erf\left[\frac{\sqrt{2}}{2}(\mu - \ln l_{\min})\right] - \frac{1}{2}erf\left[\frac{\sqrt{2}}{2}(\mu - \ln l_{\max})\right]\right\}\frac{2\,1 - e^{-\frac{\pi}{2}\lambda}()}{(\lambda^2 + 16)(1 - e^{-\frac{\pi}{2}\lambda})}$$

$$+ \frac{\nu_{LT} E_T E_L}{E_L - \nu_{LT}^2 E_T}\left\{\frac{1}{2}erf\left[\frac{\sqrt{2}}{2}(\mu - \ln l_{\min})\right] - \frac{1}{2}erf\left[\frac{\sqrt{2}}{2}(\mu - \ln l_{\max})\right]\right\}$$

$$\frac{\lambda^4 + 16\lambda^2 - 24e^{-\frac{\pi}{2}\lambda} + 24}{(\lambda^4 + 20\lambda^2 + 64)(1 - e^{-\frac{\pi}{2}\lambda})} \quad (2.95)$$

$$+ \frac{\nu_{LT} E_T E_L}{E_L - \nu_{LT}^2 E_T}\left\{\frac{1}{2}erf\left[\frac{\sqrt{2}}{2}(\mu - \ln l_{\min})\right] - \frac{1}{2}erf\left[\frac{\sqrt{2}}{2}(\mu - \ln l_{\max})\right]\right\}$$

$$\frac{24 - e^{-\frac{\pi}{2}\lambda}\lambda^4 - 16e^{-\frac{\pi}{2}\lambda}\lambda^2 - 24e^{-\frac{\pi}{2}\lambda}}{(\lambda^4 + 20\lambda^2 + 64)(1 - e^{-\frac{\pi}{2}\lambda})}$$

$$- 4G_{LT}\left\{\frac{1}{2}erf\left[\frac{\sqrt{2}}{2}(\mu - \ln l_{\min})\right] - \frac{1}{2}erf\left[\frac{\sqrt{2}}{2}(\mu - \ln l_{\max})\right]\right\}\frac{2\,1 - e^{-\frac{\pi}{2}\lambda}()}{(\lambda^2 + 16)(1 - e^{-\frac{\pi}{2}\lambda})}$$

$$
\begin{aligned}
\overline{A}_{66} = {} & \frac{E_L^2}{E_L - \nu_{LT}^2 E_T}\left\{\frac{1}{2}erf\left[\frac{\sqrt{2}}{2}(\mu - \ln l_{\min})\right] - \frac{1}{2}erf\left[\frac{\sqrt{2}}{2}(\mu - \ln l_{\max})\right]\right\}\frac{2\,1-e^{-\frac{\pi}{2}\lambda}()}{(\lambda^2+16)(1-e^{-\frac{\pi}{2}\lambda})} \\
& + \frac{E_L E_T}{E_L - \nu_{LT}^2 E_T}\left\{\frac{1}{2}erf\left[\frac{\sqrt{2}}{2}(\mu - \ln l_{\min})\right] - \frac{1}{2}erf\left[\frac{\sqrt{2}}{2}(\mu - \ln l_{\max})\right]\right\}\frac{2\,1-e^{-\frac{\pi}{2}\lambda}()}{(\lambda^2+16)(1-e^{-\frac{\pi}{2}\lambda})} \\
& - \frac{2\nu_{LT} E_T E_L}{E_L - \nu_{LT}^2 E_T}\left\{\frac{1}{2}erf\left[\frac{\sqrt{2}}{2}(\mu - \ln l_{\min})\right] - \frac{1}{2}erf\left[\frac{\sqrt{2}}{2}(\mu - \ln l_{\max})\right]\right\}\frac{2\,1-e^{-\frac{\pi}{2}\lambda}()}{(\lambda^2+16)(1-e^{-\frac{\pi}{2}\lambda})} \\
& + G_{LT}\left\{\frac{1}{2}erf\left[\frac{\sqrt{2}}{2}(\mu - \ln l_{\min})\right] - \frac{1}{2}erf\left[\frac{\sqrt{2}}{2}(\mu - \ln l_{\max})\right]\right\}\frac{\lambda^4+16\lambda^2-24e^{-\frac{\pi}{2}\lambda}+24}{(\lambda^4+20\lambda^2+64)(1-e^{-\frac{\pi}{2}\lambda})} \\
& - 2G_{LT}\left\{\frac{1}{2}erf\left[\frac{\sqrt{2}}{2}(\mu - \ln l_{\min})\right] - \frac{1}{2}erf\left[\frac{\sqrt{2}}{2}(\mu - \ln l_{\max})\right]\right\}\frac{2\,1-e^{-\frac{\pi}{2}\lambda}()}{(\lambda^2+16)(1-e^{-\frac{\pi}{2}\lambda})} \\
& + G_{LT}\left\{\frac{1}{2}erf\left[\frac{\sqrt{2}}{2}(\mu - \ln l_{\min})\right] - \frac{1}{2}erf\left[\frac{\sqrt{2}}{2}(\mu - \ln l_{\max})\right]\right\}\frac{24-e^{-\frac{\pi}{2}\lambda}\lambda^4-16e^{-\frac{\pi}{2}\lambda}\lambda^2-24e^{-\frac{\pi}{2}\lambda}}{(\lambda^4+20\lambda^2+64)(1-e^{-\frac{\pi}{2}\lambda})}
\end{aligned}
\tag{2.96}
$$

Instead of applying a constant value for the longitudinal elasticity modulus, which is calculated by inserting the modal or the mean fiber length, one may find an averaged modulus where the FLD function is included. Chin *et al.* [29] suggest that the mean longitudinal elasticity modulus could be calculated from

$$
\overline{E_L(L)} = \frac{\int_0^\infty E_L(l)\, f(l)\, dl}{\int_0^\infty f(l)\, dl}. \tag{2.97}
$$

This approach has, however, not been studied further in this report.

A third approach is applying numerical integration for the fiber length dependent part, in the same way as described for the Fu-Lauke model.

2.5.3.3 The Kacir et al model

The model by Kacir *et al.* [30] is implemented in almost the same way as the Chin *et al.* model. The only difference is the lack of the constant factor $(1-e^{-\frac{\pi}{2}\lambda})$ in the denominator of the FOD function. Because the exponential term is approaching zero for $\lambda \geq 10$, which is the value typically applied for getting the main fiber orientation in the direction of the applied load, the two models produce the same result for the effective Young's modulus for the composite.

2.6 The paper physics approach (PPA)

Cox conducted a pioneer work on what is commonly referred to as the paper physics approach (PPA) [2]. Several others have later applied and referred to this approach, see e.g. [3;38] and the references therein.

In the PPA, the key point is calculating the force across a scan line in the test specimen. This involves first calculating the number of fibers with length l and orientation θ that crosses this (imaginary) scan line. Second, the axial force in a fiber of length l and orientation θ is calculated, and the load-direction component of this force is found. Third, the calculated load-direction axial force is multiplied by the number of fibers crossing the scan line. Finally, this quantity is integrated over the fiber length and fiber orientation distribution, to calculate the total force sustained by the fibers crossing the scan line.

According to Fu and Lauke [3], which refer to the paper by Jayaraman and Kortschot [38], the elastic modulus of the short-fiber composite in the load direction can, in the context of the PPA, be expressed as,

$$\bar{E}_{11} = \chi_1 \chi_2 E_f V_f + E_m (1 - V_f) . \tag{2.98}$$

In this expression, χ_1 and χ_2 are fiber length and fiber orientation factors, respectively, and given as,

$$\chi_1 = \frac{1}{l_{\text{mean}}} \int_{l_{\min}}^{l_{\max}} \left[1 - \frac{\tanh(\beta l / 2)}{\beta l / 2} \right] l f(l) \mathrm{d}l \tag{2.99}$$

and

$$\chi_2 = \int_{\theta_{\min}}^{\theta_{\max}} \left[(\cos\theta)^2 - \nu_{LT} (\sin\theta)^2 \right] (\cos\theta)^2 g(\theta) \mathrm{d}\theta , \tag{2.100}$$

where $0 \le l_{\min} \le l \le l_{\max} \le \infty$ and $0 \le \theta_{\min} \le \theta \le \theta_{\max} \le \pi / 2$.

For illustration and for relating to the laminate-plate method in Section 2.5, we apply the same FLD and FOD functions for the PPA. In the first case, inserting the distributions functions of the Fu-Lauke model in (2.29) and (2.32), the integral expressions in (2.99) and (2.100) become

$$\chi_1 = \frac{1}{l_{\text{mean}}} \int_{l_{\min}}^{l_{\max}} \left[1 - \frac{\tanh(\beta l / 2)}{\beta l / 2} \right] a b l^b \exp(-a l^b) \mathrm{d}l \tag{2.101}$$

and

$$\chi_2 = \frac{\int_{\theta_{\min}}^{\theta_{\max}} \left[\cos^4\theta - \nu_{LT}\cos^2\theta\sin^2\theta\right]\{\sin(\theta)\}^{2p-1}\{\cos(\theta)\}^{2q-1}\mathrm{d}\theta}{\int_{\theta_{\min}}^{\theta_{\max}} \{\sin(\theta)\}^{2p-1}\{\cos(\theta)\}^{2q-1}\mathrm{d}\theta} \qquad (2.102)$$
$$= \frac{\Gamma(2+q)\Gamma(q+p)}{\Gamma(2+q+p)\Gamma(q)} - \nu_{LT}\frac{\Gamma(1+q)\Gamma(1+p)\Gamma(q+p)}{\Gamma(2+q+p)\Gamma(q)\Gamma(p)}$$

where the latter expression is based on the fact that $0 = \theta_{\min} \le \theta \le \theta_{\max} = \pi/2$, as also assumed for the Fu-Lauke model, see Section 2.5.3.1.

In the second case, applying the Chin *et al.* model in Section 2.5.3.2, the distribution functions becomes,

$$\chi_1 = \frac{1}{l_{\text{mean}}}\int_{l_{\min}}^{l_{\max}}\left[1 - \frac{\tanh(\beta l/2)}{\beta l/2}\right]\frac{1}{\sqrt{2\pi}s}\exp[-(\ln l - \mu)^2/2s^2]\mathrm{d}l \qquad (2.103)$$

and

$$\chi_2 = \frac{\int_{\theta_{\min}}^{\theta_{\max}} \left[\cos^4\theta - \nu_{12}\cos^2\theta\sin^2\theta\right]\lambda e^{-\lambda\theta}\mathrm{d}\theta}{1 - e^{-\frac{\pi}{2}\lambda}} \qquad (2.104)$$
$$= \frac{\lambda^4 + 16\lambda^2 - 24e^{-\frac{\pi}{2}\lambda} + 24}{(\lambda^4 + 20\lambda^2 + 64)(1 - e^{-\frac{\pi}{2}\lambda})} - \nu_{LT}\frac{2(1 - e^{-\frac{\pi}{2}\lambda})}{(\lambda^2 + 16)(1 - e^{-\frac{\pi}{2}\lambda})}$$

where the latter expression again is based on the fact that $0 = \theta_{\min} \le \theta \le \theta_{\max} = \pi/2$.

Both models include the Cox shear-lag function, where the value of β depends on the packing of the fibers.

3 Summary and future work

In this report, different models are described for calculating the effective modulus of randomly oriented short-fiber reinforced composite materials. The survey is not at all complete, but gives some examples on possible modeling approaches.

The overall purpose of this study is to establish a fundament for further research within the field of discontinuous fiber composites. The next step will be to apply the short-fiber model expressions to nanocomposites. If required, adjusted variants, or new models, will be established.

At this point in the study of discontinuous fiber composites, sufficient experimental tests have not been performed. This will be included in later studies.

Acknowledgements

The author would like to thank Harald Osnes (University of Oslo and FFI) and Bernt B. Johnsen (FFI) for useful discussions, reading the document, and for suggesting improvements.

References

[1] T. Thorvaldsen, B. B. Johnsen, and H. Osnes, "Modelling of nanofibre composites," *14th European Conference on Composite Materials*, 2010.

[2] H. L. Cox, "The elasticity and strength of paper and other fibrous materials," *British Journal of Applied Physics*, vol. 3, no. 3, pp. 72-79, 1952.

[3] S. Y. Fu and B. Lauke, "The elastic modulus of misaligned short-fiber-reinforced polymers," *Composites Science and Technology*, vol. 58, pp. 389-400, 1998.

[4] M. Horio and S. Onogi, "Dynamic measurements of physical properties of pulp and paper by audiofrequency sound," *Journal of Applied Physics*, vol. 22, no. 7, pp. 971-977, 1951.

[5] B. D. Agarwal, L. J. Broutman, and K. Chandrashekhara, *Analysis and performance of fiber composites*, 3rd ed John Wiley & Sons, Inc., 2006.

[6] D. Qian, E. C. Dickey, R. Andrews, and T. Rantell, "Load transfer and deformation mechanisms in carbon naonotube-polystyrene composites," *Applied Physics Letters*, vol. 76, no. 20, pp. 2868-2870, 2000.

[7] R. E. Lavengood and L. A. Goettler, "Stiffness of non-aligned fiber reinforced composites,"HPC 71-141, 1971.

[8] J. L. Kardos, "Critical issues in achieving desirable mechanical properties for short fiber composites," *Pure and Applied Chemistry*, vol. 57, no. 11, pp. 1651-1657, 1985.

[9] J. N. Coleman, U. Khan, W. J. Blau, and Y. K. Gun´ko, "Small but strong: A review of the mechanical properties of carbon nanotube-polymer composites," *Carbon*, vol. 44, pp. 1624-1652, 2006.

[10] H. Krenchel, *Fibre reinforcement* Copenhagen, Akademisk Forlag, 1964.

[11] G. P. Carman and K. L. Reifsnider, "Micromechanics of short-fiber composites," *Composites Science and Technology*, vol. 43, pp. 137-146, 1992.

[12] S. Y. Fu and B. Lauke, "Characterization of tensile behaviour of hybrid short glass fibre/calcite particle/ABS composites," *Composites: Part A*, vol. 29A, pp. 575-583, 1998.

[13] R. M. Christensen and F. M. Waals, "Effective stiffness of randomly oriented fibre composites," *Journal of Composite Materials*, vol. 6, pp. 518-532, 1972.

[14] R. M. Christensen, "Asymptotic modulus results for composites containing randomly oriented fibers," *International Journal of Solids and Structures*, vol. 12, pp. 537-544, 1976.

[15] Z. Hashin and B. W. Rosen, "The elastic moduli of fiber-reinforced materials," *Journal of Applied Mechanics*, vol. 31, pp. 223-232, 1964.

[16] Z. Hashin, "Viscoelastic fiber reinforced materials," *AIAA Journal*, vol. 4, no. 8, pp. 1411-1417, 1966.

[17] Z. Hashin, "On elastic behaviour of fibre reinforced materials of arbitrary transverse phase geometry," *Journal of the Mechanics and Physics of Solids*, vol. 13, pp. 119-134, 1965.

[18] R. Hill, "Theory of mechanical properties of fibre-strengthened materials: I. Elastic behaviour," *Journal of the Mechanics and Physics of Solids*, vol. 12, pp. 199-212, 1964.

[19] R. Hill, "Theory of mechanical properties of fibre-strengthened materials - III. self-consistent model," *Journal of the Mechanics and Physics of Solids*, vol. 13, pp. 189-198, 1965.

[20] G. J. Weng and C. T. Sun, "Effects of fiber length on elastic moduli of randomly-oriented chopped-fiber composites,". S. W. Tsai, Ed. American Society for Testing and Materials, 1979, pp. 149-162.

[21] C. T. Chon and C. T. Sun, "Stress distributions along a short fibre in fibre reinforced plastics," *Journal of Materials Science*, vol. 15, pp. 931-938, 1980.

[22] Y. Breton, G. Désarmot, J. P. Salvetat, S. Delpeux, C. Sinturel, F. Béguin, and S. Bonnamy, "Mechanical properties of multiwall carbon nanotubes/epoxy composites: influence of network morphology," *Carbon*, vol. 42, no. 5-6, pp. 1027-1030, 2004.

[23] J. D. Fidelus, E. Wiesel, F. H. Gojny, K. Schulte, and H. D. Wagner, "Thermo-mechanical properties of randomly oriented carbon/epoxy nanocomposites," *Composites: Part A*, vol. 36, pp. 1555-1561, 2005.

[24] S. Y. Fu and B. Lauke, "Effects of fiber length and fiber orientation distributions on the tensile strength of short-fiber-reinforced polymers," *Composites Science and Technology*, vol. 56, pp. 1179-1190, 1996.

[25] S. Y. Fu and B. Lauke, "The fibre pull-out energy of misaligned short fibre composites," *Journal of Materials Science*, vol. 32, pp. 1985-1993, 1997.

[26] S. Y. Fu, Z.-K. Chen, S. Hong, and C. C. Han, "The reduction of carbon nanotube (CNT) length during the manufacture of CNT/polymer composites and a method to simultaneously determine the resulting CNT and interfacial strengths," *Carbon*, vol. 47, pp. 3192-3200, 2009.

[27] M. Xia, H. Hamada, and Z. Maekawa, "Flexural stiffness of injection molded glass fiber reinforced thermoplastics," *International Polymer Processing*, vol. 10, pp. 74-81, 1995.

[28] S. Y. Fu and B. Lauke, "An analytical characterization of the anisotropy of the elastic modulus of misaligned short-fiber-reinforced polymers," *Composites Science and Technology*, vol. 58, pp. 1961-1972, 1998.

[29] W.-K. Chin, H.-T. Liu, and Y.-D. Lee, "Effects of fiber length and orientation distribution on the elastic modulus of short fiber reinforced thermoplastics," *Polymer Composites*, vol. 9, no. 1, pp. 27-35, 1988.

[30] L. Kacir, M. Narkis, and O. Ishai, "Oriented short glass-fiber composites. I. Preparation and statistical analysis of aligned fiber mats," *Polymer Engineering and Science*, vol. 15, no. 7, pp. 525-531, 1975.

[31] C. H. Chen and C. H. Cheng, "Effective elastic moduli of misoriented short-fiber composites," *International Journal of Solids and Structures*, vol. 33, no. 17, pp. 2519-2539, 1996.

[32] J. C. Halpin, "Stiffness and expansion estimates for oriented short fiber composites," *Journal of Composite Materials*, vol. 3, pp. 732-734, 1969.

[33] J. C. Halpin, K. Jerine, and J. M. Whitney, "The laminate analogy for 2 and 3 dimensional composite materials," *Journal of Composite Materials*, vol. 5, pp. 36-49, 1971.

[34] J. C. Halpin and N. J. Pagano, "The laminate approximation for randomly oriented fibrous composites," *Journal of Composite Materials*, vol. 3, no. 4, pp. 720-724, 1969.

[35] C. L. Choy, W. P. Leung, and K. W. Kowk, "Elastic moduli and thermal conductivity of injection-molded short-fiber-reinforced thermoplastics," *Polymer Composites*, vol. 13, no. 2, pp. 69-80, 1992.

[36] H. T. Hahn, "Simplified formulas for elastic moduli of unidirectional continuous fiber composites," *Journal of Composites Technology and Research*, vol. 2, no. 3, pp. 5-7, 1980.

[37] H. T. Hahn, K. L. Jernia, and K. Chiou, "Thermoelastic behavior of injection-molded thermoplastic composites," *Proceedings of the International Symposium on Composite Materials and Structures*, pp. 68-74, 1986.

[38] K. Jayaraman and M. T. Kortschot, "Correction to the Fukuda-Kawata Young's modulus theory and the Fukuda-Chou strength theory for short fibre-reinforced composite materials," *Journal of Materials Science*, vol. 31, pp. 2059-2064, 1996.